

Urology Research

Editors-in-Chief

Arnold P. P. Achermann

University of Campinas, Brazil

Yunshan Zhang

Affiliated Hospital of Guangdong Medical University, China

BIO-BYWORD SCIENTIFIC PUBLISHING PTY LTD

(619 649 400)

Level 10

50 Clarence Street

SYDNEY NSW 2000

Copyright © 2025. Bio-Byword Scientific Publishing Pty Ltd.

Complimentary Copy



Urology Research

Focus and Scope

Urology Research publishes peer-reviewed research articles across basic, translational, and clinical Urology medicine. The Journal covers all aspects of Urology medicine (full listing below) with an emphasis on studies that challenge the status quo of treatments and practices in Urology care or facilitate the translation of scientific advances into the clinic as new therapies or diagnostic tools.

About Publisher

Bio-Byword Scientific Publishing is a fast-growing, peer-reviewed and open access journal publisher, which is located in Sydney, Australia. As a dependable and credible corporation, it promotes and serves a broad range of subject areas for the benefit of humanity. By informing and educating a global community of scholars, practitioners, researchers and students, it endeavors to be the world's leading independent academic and professional publisher. To realize it, it keeps creative and innovative to meet the range of the authors' needs and publish the best of their work.

By cooperating with University of Sydney, University of New South Wales and other world-famous universities, Bio-Byword Scientific Publishing has established a huge publishing system based on hundreds of academic programs, and with a variety of journals in the subjects of medicine, construction, education and electronics.

Publisher Headquarter

BIO-BYWORD SCIENTIFIC PUBLISHING PTY LTD

Level 10

50 Clarence Street

Sydney NSW 2000

Website: www.bbwpublisher.com

Email: info@bbwpublisher.com

Table of Contents

- 1 Efficacy and Safety of Firsekibart in Gout Patients with Different Estimated Glomerular Filtration Rates**
Yu Xue, Yi Li, Yuling Lian, Fei Gu, Chunxia Chen, Qian Xu
- 13 The Roles of E2F5 in Tumor Cell Cycle: The Gatekeeper or Destroyer?**
Yingwen Du, Danyun Wang, Aidi Liang, Xinru Tang, Jiansen Chen, Ruizhi Yao, Lei Meng, Jianxing Xie, Ming Chen, Songtao Xiang, Canbin Lin
- 25 Multivariable Mendelian Randomization Analysis Reveals Potential Causal Effects between Immune Cells and Prostate Cancer Risk**
Bin Hu, Haiqin Luo, Zhangcheng Liu
- 38 The Effect of Body Temperature Flush Solution on Patients Undergoing Holmium Laser Lithotripsy via Ureteroscopy**
Ming Xiong

Efficacy and Safety of Firsekibart in Gout Patients with Different Estimated Glomerular Filtration Rates

Yu Xue^{1*}, Yi Li², Yuling Lian², Fei Gu², Chunxia Chen², Qian Xu²

¹Department of Rheumatology, Huashan Hospital, Fudan University, Shanghai 200040, China

²Changchun GeneScience Pharmaceutical Co., Ltd. Changchun 130000, Jilin, China

*Corresponding author: Yu Xue, xueyu20242024@163.com

Copyright: © 2025 Author(s). This is an open-access article distributed under the terms of the Creative Commons Attribution License (CC BY 4.0), permitting distribution and reproduction in any medium, provided the original work is cited.

Abstract: *Objective:* To compare the efficacy and safety of Firsekibart versus compound betamethasone in gout patients with different estimated glomerular filtration rate (eGFR) levels. *Methods:* Patients were randomized 1:1 to receive a single dose of Firsekibart (200 mg) or Compound betamethasone (7mg). Patients were divided into three subgroups according to baseline eGFR: ≥ 90 , 60-89, and 30-59 ml/min/1.73 m² to evaluate 72-hour pain relief, 12/24-week recurrence rate, renal function changes, and safety events. *Results:* Of 311 patients in full analysis set (FAS), 113 (36.3%) had baseline eGFR 60-89 ml/min/1.73 m², and 42 (13.5%) had baseline eGFR 30-59 ml/min/1.73 m². Similar reduction in visual analogue scale (VAS) scores at 72-hour was observed in each eGFR subgroup between Firsekibart and compound betamethasone group ($P > 0.05$). Compared with Compound betamethasone, Firsekibart reduced the risk of recurrence at 12/24 weeks in patients with different eGFR subgroups (all $P < 0.0001$). In safety evaluation, no obvious changes of creatinine and eGFR were observed in each subgroup during 24-week follow up. Treatment emergent adverse events (TEAEs) incidence was comparable in each eGFR subgroup analysis. In total, 1 (0.6%) treatment-emergent serious adverse events (TESAE) and 0 treatment-related adverse events (TRSAE) occurred in the Firsekibart group compared to 6 (3.8%) and 3 (1.9%) in the Compound betamethasone group, respectively. *Conclusion:* Overall, Firsekibart demonstrated non-inferior short-term pain relief while offering better prevention of new flares, with a lower incidence of serious adverse events compared to compound betamethasone, and results were consistent across eGFR subgroups. Both Firsekibart and compound betamethasone showed little effect on renal function.

Keywords: Acute gouty arthritis; Chronic kidney disease; Inflammation; Firsekibart; Compound betamethasone

Online publication: Oct 17, 2025

1. Introduction

When the concentration of uric acid in the blood exceeds its dissolution limit, monosodium urate crystals are formed and deposited in the joints and surrounding tissues, inducing acute inflammatory reactions, resulting in gout attacks^[1]. Acute gouty arthritis (AGA) is the core clinical manifestation of gout. According to statistics, the global incidence of gout increased from 93.10/100,000 to 109.08/100,000 from 1990 to 2021, and the incidence rate in China increased from 122.52/100,000 to 151.61/100,000 during the same period^[2]. Hyperuricemia is

an important factor in the development and prognosis of chronic kidney disease (CKD)^[1]. Kidney disease is common in gout patients, about 71% of adult gout patients accompany with glomerular filtration rate (eGFR) $<60 \text{ mL/min/1.73 m}^2$ ^[3], and 20% with eGFR $<30 \text{ mL/min/1.73 m}^2$. Hyperuricemia in patients with gout can accelerate kidney damage, and decreased renal function can aggravate uric acid accumulation, leading to recurrent gout and significantly increasing the difficulty of treatment^[4].

Glucocorticoids are routinely administered during acute gout attacks, especially when patients present with systemic symptoms or when colchicine and nonsteroidal anti-inflammatory drugs (NSAIDs) are ineffective, contraindicated, or renal insufficiency^[5]. Despite the powerful anti-inflammatory and immunosuppressive effects of glucocorticoids, they are widely used to treat a variety of immune-mediated inflammatory diseases. However, glucocorticoids have serious side effects, and long-term use can increase the risk of infection in patients, leading to complications such as insulin resistance and osteoporosis^[6].

Interleukin-1 β (IL-1 β) is a pro-inflammatory factor produced and released by a variety of cells in response to inflammatory signals, participating in a variety of autoimmune inflammatory responses, and is also an important target of anti-inflammatory therapy. In the gout inflammatory response, IL-1 β drives gout attacks by activating endothelial cells, releasing inflammatory factors, and recruiting neutrophils^[7-10]. IL-1 β acts as a key effector protein in the NLR family pyrin domain containing protein 3 (NLRP3) pathway, mediating renal fibrosis in CKD^[11, 12]. IL-1 β inhibitors are more selective than glucocorticoids and have fewer expected side effects while effective. Targeted inhibition of IL-1 β can not only control the gout inflammatory response, but may also provide renal protection for patients with CKD.

Firsekibart is a new fully human monoclonal antibody independently developed in China, and has a high affinity for IL-1 β ^[13], and showed great efficacy and safety in treating gout^[13]. However, the effect of Firsekibart in gout patients with CKD has not been reported. Therefore, we made an post-hoc subgroup analysis of Firsekibart in patients with different baseline eGFRs.

2. Methods

2.1. Study design and patient population

This study was a multicenter, randomized, double-blind, double-dummy, positive-controlled phase III clinical trial conducted in 51 centers in China, including patients with contraindications, intolerance, insufficient efficacy of NSAIDs and/or colchicine, and recurrent attacks of acute gout from January 2023 to June 2024. Key inclusion criteria included: age 18 to 75 years; body mass index (BMI) $\leq 40 \text{ kg/m}^2$, meeting the American College of Rheumatology 2015 classification criteria for gout^[14]; ≥ 2 episodes of acute gout in the prior 1 year; contraindications, intolerance, or poor efficacy to NSAIDs and/or colchicine. Key exclusion criteria included: allergy to the study drug or similar drugs; use of prohibited medications within a specific time prior to screening (such as NSAIDs, and colchicine); eGFR $< 30 \text{ mL/min/1.73 m}^2$, diseases that may interfere with joint assessment (such as rheumatoid arthritis); history of severe immunodeficiency and severe comorbidities.

The study was approved by the ethical review committees of all participating centers. All patients signed an informed consent form prior to enrollment. Study registration numbers: NCT05983445 and CTR20223136.

2.2. Data collection

Demographic data, clinical manifestations, and laboratory examination data were collected by electronic data acquisition system. In this post-hoc article, patients were divided into three groups based on baseline eGFR,;

eGFR ≥ 90 mL/min/1.73 m²; eGFR 60-89 mL/min/1.73 m²; and eGFR 30-59 mL/min/1.73 m²^[15]. Key follow-up index included: the change in pain intensity from baseline to 72 hours, recurrence time within 12/24 weeks, and renal function measurements at Day 8, 4 and 24 weeks after drug administration.

2.3. Treatment regimen

Patients were randomized in a 1:1 ratio to receive a single dose Firsekibart (200mg) or compound betamethasone(7mg) using a stratified block randomization method, with pain intensity at screening ($50 \leq \text{VAS} < 70$ mm vs. $70 \leq \text{VAS} < 100$ mm) as the stratification factor. The study was designed by a 24-week of double-blind core studies treatment followed by another 24-week open-label extension, and a 12-week safety follow-up since last dose. During the double-blind period, patients who experienced a subsequent flare would require re-treatment with the same study drug with a time interval of >14 days between doses.

2.4. Efficacy and safety evaluation

Change in the VAS pain score of the target joint, time to first new flare within 12/24 weeks, proportion of patients experiencing at least 1 new flare and the mean number of flares per patient over 12/24 weeks were measured to evaluate the efficacy. Besides, we used change in creatinine and eGFR to evaluate the influence on the renal function and the incidence of adverse events to evaluate the overall safety. Safety assessments were classified according to the common terminology Criteria for Adverse Events, version 5.0. The occurrence of adverse events in each subgroup during the study period was recorded.

2.5. Statistical analysis

Categorical data were presented as numbers and percentages. Continuous variables are presented as means with standard deviations or medians with quartiles (quartile 1 [Q1], quartile 3 [Q3]). The full analysis set (FAS), which included all randomized patients who received at least 1 dose of the study drug and had at least 1 post-treatment efficacy assessment, was used for the analysis of VAS scores and recurrence. The safety set (SS), which included all randomized patients who received at least 1 dose of the study drug and had safety assessments, was used for the analysis of renal function and

For the change in pain intensity at 72 h post-dose, a non-inferiority test was conducted using a mixed-effects model for repeated measures. The model included baseline VAS score as a covariate, treatment group, assessment time points, and the interaction between treatment group and time points as fixed effects. For the time to first new flare within 12 weeks after treatment, HR of the Firsekibart versus Compound betamethasone group was estimated with stratified Cox proportional hazards model using the prespecified stratification factors at randomization. The median time to flare and corresponding 95% CI for each group were estimated with the Kaplan-Meier method.

3. Outcomes

3.1. Baseline characteristics

A total of 311 patients (156 in the Firsekibart group and 155 in the Compound betamethasone group) were included in full analysis set (FAS). Baseline demographics and disease characteristics were generally comparable between groups (Table 1).

Table 1. Baseline data

| | Firsekibart group(N = 156) | | | | Compound betamethasone group(N = 155) | | | |
|---|--|--|--|--------------------|--|--|--|--------------------|
| | ≥ 90 mL/ min/1.73 m ² (N = 76) | 60–89 mL/ min/1.73 m ² (N = 59) | 30–59 mL/ min/1.73 m ² (N = 21) | Total (N = 156) | ≥ 90 mL/ min/1.73 m ² (N = 80) | 60–89 mL/ min/1.73 m ² (N = 54) | 30–59 mL/ min/1.73 m ² (N = 21) | Total (N = 155) |
| Male, n (%) | 76 (100) | 59 (100) | 21 (100) | 156 (100) | 79 (98.8) | 52 (96.3) | 20 (95.2) | 151 (97.4) |
| Age, Years, Mean (SD) | 39.0 (11.87) | 49.6 (12.36) | 58.8 (9.58) | 45.7 (13.73) | 39.0 (9.99) | 47.3 (12.84) | 55.4 (6.66) | 44.1 (12.16) |
| BMI (kg/m ²), mean (SD) | 28.00 (4.013) | 27.19 (3.960) | 26.17 (2.831) | 27.45 (3.885) | 28.20 (4.290) | 26.84 (3.197) | 26.91 (2.692) | 27.55 (3.788) |
| Number of flares in prior 1 year, n (%) | | | | | | | | |
| 2 flares | 7 (9.2) | 5 (8.5) | 1 (4.8) | 13 (8.3) | 14 (17.5) | 5 (9.3) | 1 (4.8) | 20 (12.9) |
| 3–5 flares | 38 (50.0) | 28 (47.5) | 7 (33.3) | 73 (46.8) | 35 (43.8) | 25 (46.3) | 9 (42.9) | 69 (44.5) |
| 6–12 flares | 24 (31.6) | 23 (39.0) | 9 (42.9) | 56 (35.9) | 25 (31.3) | 15 (27.8) | 7 (33.3) | 47 (30.3) |
| > 12 flares | 7 (9.2) | 3 (5.1) | 4 (19.0) | 14 (9.0) | 6 (7.5) | 9 (16.7) | 4 (19.0) | 19 (12.3) |
| Presence of gouty tophi, n (%) | 22 (28.9) | 28 (47.5) | 11 (52.4) | 61 (39.1) | 30 (37.5) | 25 (46.3) | 10 (47.6) | 65 (41.9) |

eGFR: estimated glomerular filtration rate; BMI: body mass index

3.2.VAS scores analysis of patients with different baseline eGFRs

In total, VAS scores changes from baseline to 72h post-dose in Firsekibart and Compound betamethasone groups were -57.09 mm and -53.77 mm, respectively, with a difference of -3.32mm

(95%CI:-7.561 to 0.914).In patients with baseline eGFR ≥ 90 ml/min/1.73 m², the VAS scores changes from baseline to 72h post-dose in Firsekibart and Compound betamethasone groups were -56.42 mm and -53.74 mm, respectively, with a difference of -2.68 mm (95% CI: -8.949 to 3.594). In the patients with baseline eGFR of 60-89 ml/min/1.73 m², the VAS scores changes from baseline to 72h post-dose in Firsekibart and Compound betamethasone groups were -57.72 mm and -51.82 mm, with a difference of -5.90mm (95% CI: -12.401 to 0.602). In patients with a baseline eGFR of 30-59 ml/min/1.73 m², the VAS scores changes from baseline to 72h post-dose in Firsekibart and Compound betamethasone groups were -58.22mm and -58.33mm, respectively, with a difference of 0.11 mm (95% CI: -13.115 to 13.329) (**Table 2**). As the upper bound of the 95% CI was below the 10 mm, Firsekibart showed non-inferiority on pain relief, and consistent trend was seen in different eGFR subgroup.

3.3. Recurrence analysis of patients with different baseline eGFR

The median time to first new flare was not reached within 12 weeks in the Firsekibart group within different baseline eGFRs, while in compound betamethasone group, it was 82 days in patients with baseline eGFR of ≥ 90 ml/min/1.73 m², 30.5 days in the patients with baseline eGFR of ≥ 60 -89 ml/min/1.73 m², and 21.0 days in patients with a baseline eGFR of 30-59 ml/min/1.73 m².

Compared with compound betamethasone, lower recurrence rate was seen in Firsekibart group . By week 12, in patients with baseline eGFR of ≥ 90 ml/min/1.73 m²,10.64% patients in the Firsekibart group experienced ≥ 1 acute flare compared with 51.59% patients in the compound betamethasone group. Consistent results were shown in patients with baseline eGFR of ≥ 60 -89 and 30-59 ml/min/1.73 m² (13.56% vs 77.78%, 4.76% vs 95.24%).

Compared with the compound betamethasone, Firsekibart reduced the 12-week risk of new flare in patients with different baseline eGFRs (≥ 90 mL/min/1.73 m²: hazard ratio (HR)=0.15, 95% CI: 0.072 to 0.329, $P<0.0001$; 60-89 mL/min/1.73 m²: HR=0.09, 95% CI: 0.042 to 0.194, $P<0.0001$; 30-59 mL/min/1.73 m²: HR=0.02, 95% CI: 0.003 to 0.158, $P=0.0002$). Consistent results were seen within 24 weeks(**Table 3, Figure**

1). These results indicated that compared with compound betamethasone, Firsekibart reduced the risk of acute gout recurrence within 12 and 24 weeks in different renal function situation

Table 2. VAS scores changes from baseline to 72 h in the full analysis set

| Baseline eGFR | Variables | Fiese kibart group(N = 156) | CB group(N = 155) |
|----------------------------------|---|--------------------------------|------------------------------|
| Total | Change from baseline (mm), LSM (95% CI) | -57.09 (-60.082, -54.098) | -53.77 (-56.767, -50.765) |
| | Treatment difference (mm) LSM (95% CI) | -3.32 (95%CI:-7.561, 0.914) | |
| ≥ 90 mL/min/1.73 m ² | Change from baseline (mm), LSM (95% CI) | -56.42 (-60.911, -51.928) | -53.74 (-58.118, -49.366) |
| | Treatment difference (mm) LSM (95% CI) | -2.68 (-8.949, 3.594) | |
| 60–89 mL/min/1.73 m ² | Change from baseline (mm), LSM (95% CI) | -57.72 (-62.209, -53.227) | -51.82 (-56.515, -47.122) |
| | Treatment difference (mm) LSM (95% CI) | -5.90 (-12.401, 0.602) | |
| 30–59 mL/min/1.73 m ² | Change from baseline (mm), LSM (95% CI) | -58.22 (-67.516, -48.927) | -58.33 (-67.635, -49.022) |
| | Treatment difference (mm) LSM (95% CI) | 0.11 (-13.115, 13.329) | |

CB: Compound betamethasone, eGFR: estimated glomerular filtration rate; CI: confidence interval, LSM: least squares mean

Table 3. Recurrence analysis in in the full analysis set

| Baseline eGFR | Variables | Fiese kibart group (N = 156) | CB group (N = 155) | HR (95% CI) compared to CB group | p-value |
|----------------------------------|---|------------------------------|---------------------------|----------------------------------|----------|
| ≥ 90 mL/min/1.73 m ² | Time to first acute gout flare within 12 weeks (days) Median (95% CI) | NR (NE, NE) | 82.0 (48.00, -) | 0.15 (0.072 0.329) | < 0.0001 |
| | Recurrence rate (%) (95% CI) | 10.64 (5.466, 20.151) | 51.59 (41.153, 62.930) | | |
| | Time to first acute gout flare within 24 weeks (days) Median (95% CI) | NR (NE, NE) | 82.0 (48.00, -) | 0.21 (0.113, 0.408) | < 0.0001 |
| | Recurrence rate (%) (95% CI) | 24.23 (10.675, 49.448) | 54.75 (44.063, 66.113) | | |
| 60–89 mL/min/1.73 m ² | Time to first acute gout flare within 12 weeks (days) Median (95% CI) | NR (NE, NE) | 30.5 (24.00, 55.00) | 0.09 (0.042, 0.194) | < 0.0001 |
| | Recurrence rate (%) (95% CI) | 13.56 (7.024, 25.289) | 77.78 (66.021, 87.703) | | |
| | Time to first acute gout flare within 24 weeks (days) Median (95% CI) | NR (NE, NE) | 30.5 (24.00, 55.00) | 0.11 (0.051, 0.220) | < 0.0001 |
| | Recurrence rate (%) (95% CI) | 15.25 (8.246, 27.265) | 75.93 (63.980, 86.275) | | |
| 30–59 mL/min/1.73 m ² | Time to first acute gout flare within 12 weeks (days) Median (95% CI) | NR (NE, NE) | 21.0 (15.00, 29.00) | 0.02 (0.003, 0.158) | 0.0002 |
| | Recurrence rate (%) (95% CI) | 4.76 (0.685, 29.279) | 95.24 (80.296, 99.668) | | |
| | Time to first acute gout flare within 24 weeks (days) Median (95% CI) | NR (NE, NE) | 21.5 (15.00, 29.00) | 0.04 (0.008, 0.167) | < 0.0001 |
| | Recurrence rate (%) (95% CI) | 9.52 (2.471, 32.995) | 95.00 (79.470, 99.655) | | |

CB: Compound betamethasone, eGFR: estimated glomerular filtration rate; HR: risk ratio; 95% CI: 95% confidence interval

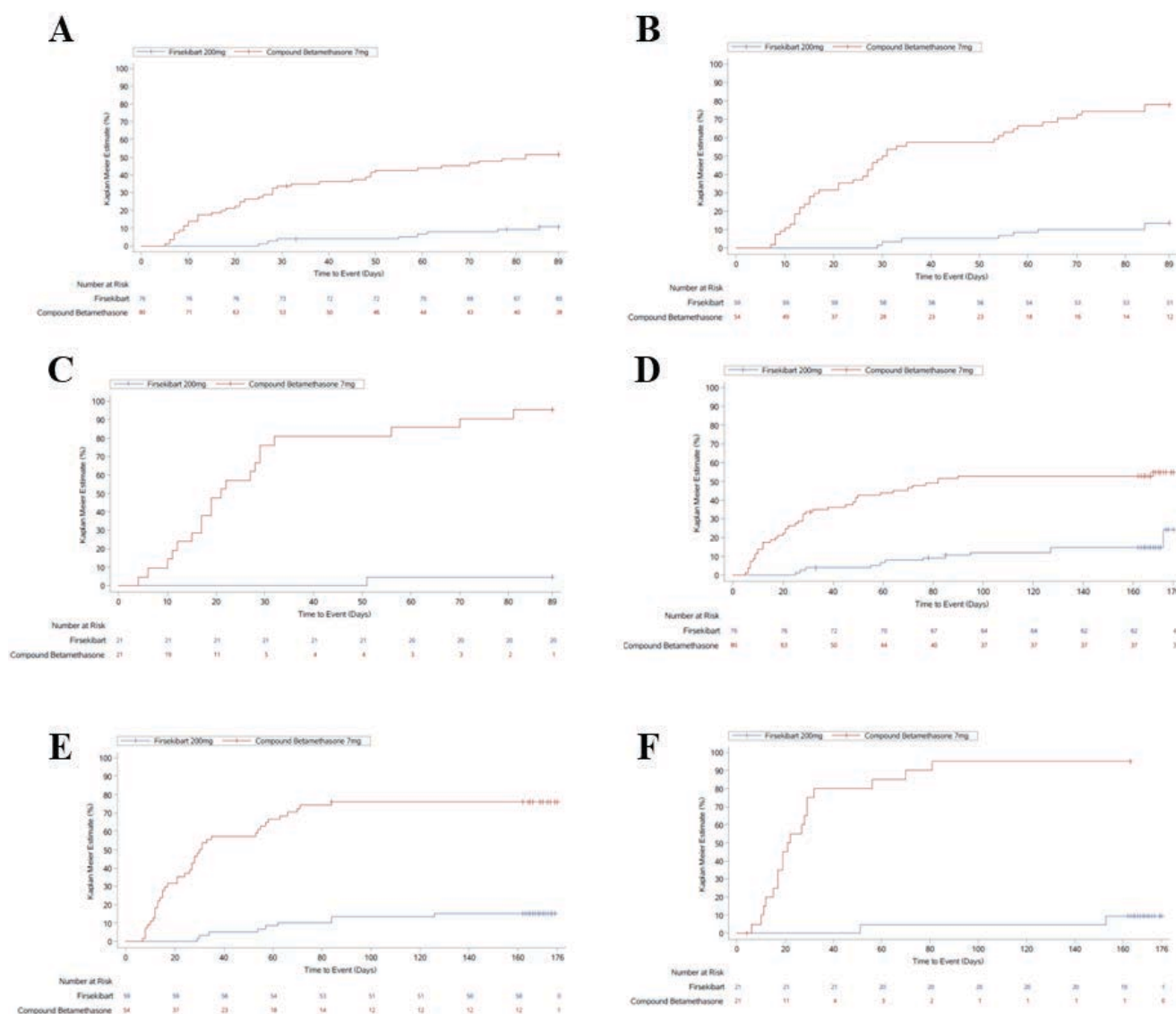


Figure 1. Kaplan-Meier curve of time to first acute gout flare within 12/24 weeks with different eGFR groups in the full analysis set A-C: Kaplan-Meier curve of time to first acute gout flare within 12weeks in eGFR: ≥ 90 , 60-89, and 30-59 mL/min/1.73 m². D-F: Kaplan-Meier curve of time to first acute gout flare within 24 weeks in eGFR: ≥ 90 , 60-89, and 30-59 mL/min/1.73 m².

3.4. Renal function analysis of patients with different baseline eGFR

A total of 312 patients (156 in the Firsekibart group and 156 in the Compound betamethasone group) were included in safety set (SS). The creatinine and eGFR were stable during 24-week observation in Firsekibart group (**Figure 2**). The changes in eGFR was $-6.407 \sim 3.520$ mL/min/1.73 m² (least squares mean) in the Firsekibart group with different eGFR stratification at multiple time observation points within 24 weeks (**Table 4**). Progression to stage 4 kidney disease (eGFR < 30 mL/min/1.73 m²) was rare and just occurred in 1 (0.64%) patient of Firsekibart group.

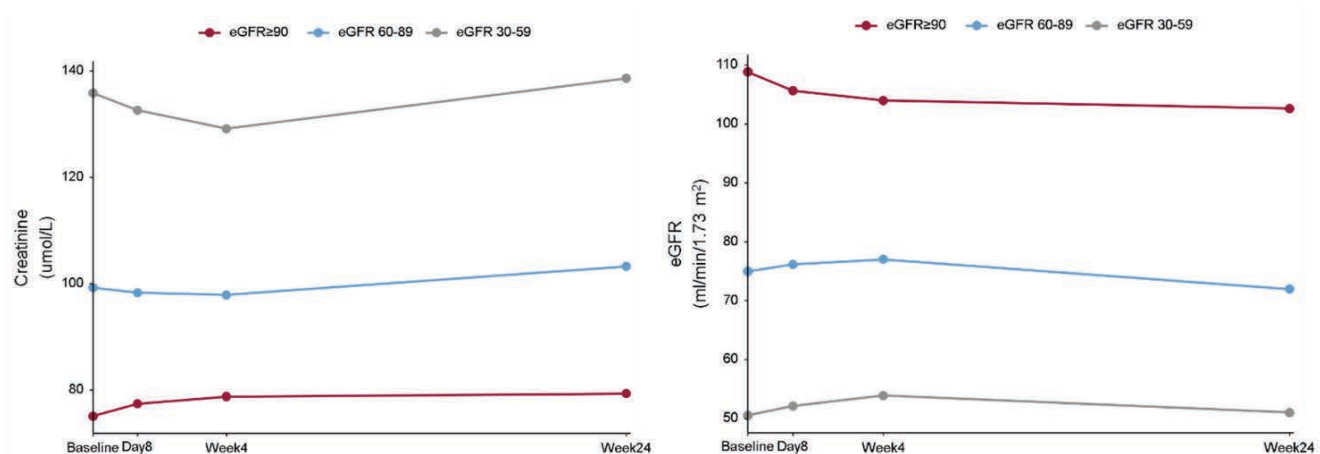


Figure 2. Effects of Firsiekibart on creatinine and eGFR in safety set.

Table 4. Changes in creatinine and eGFR in safety set

| Baseline eGFR | Variables | Firsiekibart group (N = 156) | CB group (N = 156) | Difference |
|----------------------------------|------------------------------------|------------------------------|--------------------|------------------------|
| ≥ 90 mL/min/1.73 m ² | Day 8 - baseline | | | |
| | Creatinine (umol/L) | 2.483 | 1.612 | 0.870 |
| | LSM (95% CI) | (0.717, 4.248) | (-0.109, 3.333) | (-1.599, 3.340) |
| | eGFR (mL/min/1.73 m ²) | -3.486 | -2.184 | -1.302 |
| | LSM (95% CI) | (-6.273, -0.699) | (-4.900, 0.532) | (-5.199, 2.595) |
| | Week 4 - baseline | | | |
| | Creatinine (umol/L) | 3.844 | 1.169 | 2.675 |
| | LSM (95% CI) | (1.842, 5.846) | (-0.902, 3.241) | (-0.212, 5.562) |
| | eGFR (mL/min/1.73 m ²) | -5.059 | -0.850 | -4.209 |
| | LSM (95% CI) | (-8.322, -1.796) | (-4.227, 2.526) | (-8.912, 0.494) |
| | Week 24 - baseline | | | |
| | Creatinine (umol/L) | 4.525 | 2.400 | 2.125 |
| | LSM (95% CI) | (2.478, 6.573) | (0.381, 4.419) | (-0.758, 5.008) |
| | eGFR (mL/min/1.73 m ²) | -6.407 | -3.382 | -3.025 |
| | LSM (95% CI) | (-9.621, -3.193) | (-6.552, -0.212) | (-7.551, 1.501) |
| 60–89 mL/min/1.73 m ² | Day 8 - baseline | | | |
| | Creatinine (umol/L) | -0.629 | -1.785 | 1.156 |
| | LSM (95% CI) | (-2.891, 1.633) | (-4.150, 0.580) | (-2.126, 4.439) |
| | eGFR (mL/min/1.73 m ²) | 1.073 | 1.989 | -0.916 (-4.091, 2.259) |
| | LSM (95% CI) | (-1.115, 3.260) | (-0.298, 4.275) | |
| | Week 4 - baseline | | | |
| | Creatinine (umol/L) | -1.035 | 1.513 | -2.548 |
| | LSM (95% CI) | (-4.061, 1.990) | (-1.996, 5.022) | (-7.207, 2.111) |
| | eGFR (mL/min/1.73 m ²) | 2.003 | -0.508 | 2.510 |
| | LSM (95% CI) | (-0.692, 4.698) | (-3.634, 2.619) | (-1.642, 6.663) |
| | Week 24 - baseline | | | |
| | Creatinine (umol/L) | 4.407 | -3.664 | 8.071 |
| | LSM (95% CI) | (1.421, 7.393) | (-6.909, -0.419) | (3.652, 12.490) |
| | eGFR (mL/min/1.73 m ²) | -3.350 | 4.414 | -7.764 |
| | LSM (95% CI) | (-5.987, -0.713) | (1.548, 7.280) | (-11.672, -3.856) |

Table 4 (Continued)

| Baseline eGFR | Variables | Fiesekibart group (N = 156) | CB group (N = 156) | Difference |
|----------------------------------|------------------------------------|-----------------------------|--------------------------|-------------------------|
| 30–59 mL/min/1.73 m ² | | | | |
| | | Day 8 - baseline | | |
| | Creatinine (umol/L) | -3.555 | -3.125 | -0.430 |
| | LSM (95% CI) | (-9.949, 2.839) | (-9.678, 3.429) | (-9.642, 8.782) |
| | eGFR (mL/min/1.73 m ²) | 1.546 (-1.180, 4.272) | 2.411 (-0.382, 5.205) | -0.865 (-4.794, 3.064) |
| | LSM (95% CI) | | | |
| | | Week 4 - baseline | | |
| | Creatinine(umol/L) | -7.177 | -10.063 (-20.786, 0.660) | 2.886 (-10.795, 16.568) |
| | LSM (95% CI) | (-15.600, 1.246) | | |
| | eGFR (mL/min/1.73 m ²) | 3.520 (-0.670, 7.710) | 6.164 | -2.645 (-9.479, 4.190) |
| | LSM (95% CI) | | (0.821, 11.507) | |
| | | Week 24 - baseline | | |
| | Creatinine(umol/L) | 2.124 | -11.024 | 13.148 |
| | LSM (95% CI) | (-9.513, 13.760) | (-22.951, 0.903) | (-3.617, 29.913) |
| | eGFR (mL/min/1.73 m ²) | 0.569 (-3.627, 4.764) | 6.112 | -5.543 |
| | LSM (95% CI) | | (1.811, 10.412) | (-11.592, 0.505) |

CB: Compound betamethasone, eGFR: estimated glomerular filtration rate; CI: confidence interval, LSM: Least squares mean

3.5. Adverse events analysis of patients with different baseline eGFR

The overall incidence of treatment-emergent adverse events (TEAEs) was comparable between groups, occurring in 111 patients (71.2%; grade ≥ 3 , 12.2%) in the Fiesekibart group and 109 patients (69.9%; grade ≥ 3 , 10.9%) in the compound betamethasone group. Treatment-related adverse events (TRAEs) were reported in 79 patients (50.6%; grade ≥ 3 , 10.9%) receiving Fiesekibart and 80 patients (51.3%; grade ≥ 3 , 5.1%) receiving compound betamethasone. Compared with compound betamethasone, Patients in Fiesekibart group experienced less treatment-emergent serious adverse events (TESAE) (1(0.6%) vs 6 (3.8%)). All 3 treatment-related serious adverse events (TRSAE) cases occurred in the Compound betamethasone group. The adverse events in different eGFR stratification were shown in **Table 5**.

Table 5. Adverse events in safety set

| | Fiesekibart group (N = 156) | | | | CB group (N = 156) | | | |
|-------------------------------|--|--|--|--------------------|--|--|--|--------------------|
| | ≥ 90 mL/ min/1.73 m ² (N = 76) | 60–89 mL/ min/1.73 m ² (N = 59) | 30–59 mL/ min/1.73 m ² (N = 21) | Total (N = 156) | ≥ 90 mL/ min/1.73 m ² (N = 80) | 60–89 mL/ min/1.73 m ² (N = 55) | 30–59 mL/ min/1.73 m ² (N = 21) | Total (N = 156) |
| TEAE (%) | 59 (77.6) | 42 (71.2) | 10 (47.6) | 111 (71.2) | 60 (75.0) | 38 (69.1) | 11 (52.4) | 109 (69.9) |
| TRAE (%) | 46 (60.5) | 26 (44.1) | 7 (33.3) | 79 (50.6) | 45 (56.3) | 29 (52.7) | 6 (28.6) | 80 (51.3) |
| Grade ≥ 3 of TEAE (%) | 12 (15.8) | 6 (10.2) | 1 (4.8) | 19 (12.2) | 12 (15.0) | 3 (5.5) | 2 (9.5) | 17 (10.9) |
| Grade ≥ 3 of TRAE (%) | 12 (15.8) | 4 (6.8) | 1 (4.8) | 17 (10.9) | 5 (6.3) | 3 (5.5) | 0 | 8 (5.1) |
| TESAE (%) | 0 | 1 (1.7) | 0 | 1 (0.6) | 3 (3.8) | 3 (5.5) | 0 | 6 (3.8) |
| TRSAE (%) | 0 | 0 | 0 | 0 | 0 | 3 (5.5) | 0 | 3 (1.9) |

CB: Compound betamethasone, eGFR: estimated glomerular filtration rate; TEAE: treatment-emergent adverse events; TRAE: treatment-related adverse events; TESAE: treatment-emergent serious adverse events; TRSAE: treatment-related serious adverse events

4. Discussion

In this study, the pain relief efficacy of Firsekibart was comparable to that of compound betamethasone at 72 hours in patients with different baseline eGFRs. Besides, compared with compound betamethasone, Firsekibart reduced the recurrence risk of gout over 12/24 weeks. In the evaluation of renal function, creatinine and eGFR were stable during 24-week observation in Firsekibart group. In the evaluation of adverse events, there was no obvious difference in the overall incidence of TEAEs between Firsekibart and Compound betamethasone, and patients in Firsekibart group experienced less TESAE and TRSAEs, indicating that Firsekibart had a favorable safety profile. These results support that Firsekibart has better efficacy than Compound betamethasone in gout patients with CKD without worsening renal function, and its long-term use may offer a higher safety profile than compound betamethasone.

Recurrent gout flare can lead to multisystem damage through persistent inflammatory responses and monosodium urate crystal deposition, including irreversible joint destruction, secondary tophi infection, and increased risk of acute cardiovascular events^[16]. Studies have shown enhanced renal medullary echogenicity in patients with severe gout, possibly due to sodium urate crystallization and the formation of stones within the renal medulla^[17], suggesting that sodium urate crystal-driven inflammation may directly affect kidney structure and function in patients with gout^[18]. An prospective study including 0.5 million adults showed frequent gout flares (≥ 2) greater elevated risks for CKD-HR compared to no gout=10.95 than single gout flare(HR compared to no gout=3.01)^[19]. Therefore, preventing recurrent gout attacks is crucial for the treatment of patients with gout and CKD. The current study confirmed that Firsekibart reduced the risk of gout recurrence, and this advantage was consistent in patients with different stages of CKD. These results suggest that the efficacy of Firsekibart in preventing gout flare can also benefit kidney.

According to the 2024 edition of the “Clinical Practice Guidelines for the Assessment and Management of Chronic Kidney Disease” released by KDIGO, a global kidney disease prognosis organization, when conducting risk assessment for CKD patients, if the eGFR changes in CKD patients occur in follow-up testing $> 20\%$ exceeding expectations, further attention and evaluation are needed^[20]. In the present study, patients with different baseline eGFRs in both groups experienced small fluctuations in eGFR at different times after treatment. The changes in eGFR from the baseline was $-6.407 \sim 3.520$ ml/min/1.73 m² in the Firsekibart group and $-3.382 \sim 6.164$ ml/min/1.73 m² the Compound betamethasone group, which did not meet the criteria indicating a significant change in CKD patient. Therefore, neither compound betamethasone nor Firsekibart showed any adverse effects on kidney function in this study.

Colchicine and NSAIDs are the first-line drugs for treating gout attacks, and glucocorticoid can also be considered when there are contraindications or poor treatment effect for colchicine/ NSAIDs^[5]. However, these drugs need to be used with greater caution in patients with CKD. Colchicine treatment may cause gastrointestinal adverse reactions, liver and kidney damage, and bone marrow suppression, and regular monitoring of liver and kidney function and routine blood tests are required^[5]. NSAIDs may have adverse effects on the kidneys, including acute and chronic renal failure, nephrotic syndrome with interstitial nephritis, papillary necrosis, and decreased potassium and sodium excretion^[21]. Glucocorticoids are commonly used for gout patients with CKD, but long-term use can cause significant side effects such as glucolipid metabolism disorders, increased risk of infection, and osteoporosis^[6]. Firsekibart is a novel, fully human anti-interleukin-1 β monoclonal antibody, which does not excrete through the kidneys in its original form, making it a potentially better choice for gout patients with CKD.

Anti-inflammatory therapy is vital to reducing gout attacks and kidney damage. Sodium urate crystals formed during hyperuricemia initiate gout by activating monocytes and macrophages. IL-1 β released after macrophage activation can cause infiltration and activation of joint neutrophils, leading to other local and systemic inflammatory responses^[22]. There is a bidirectional relationship between IL-1 β and monocytes/macrophages, which are the main source of IL-1 β , which in turn activates macrophages. IL-1 β also stimulates the release of other inflammatory cytokines such as tumor necrosis factor α (TNF- α) and interleukin-6 (IL-6) by activating the nuclear factor κ B (NF- κ B) pathway, causing local inflammation and kidney damage^[23]. In addition, uric acid itself activates the immune system, and uric acid from nucleosides released in dead cells has been shown to have a significant promoting effect on inflammatory responses in the body^[24]. In the kidney, urate-induced activation of NLRP3 inflammasomes and release of IL-1 β promote chemokine signaling in proximal tubular cells, leading to tubular damage and proteinuria, which in turn promotes intrarenal inflammation, interstitial fibrosis, and the development of chronic kidney disease^[25]. Therefore, anti-inflammatory therapy, especially targeting IL-1 β as a key effector in the inflammatory response, can alleviate tissue damage caused by hyperuricemia and urate crystallization at the pathological level. This also provides the theoretical foundation for the treatment effects of Firsekibart in gout patients with CKD.

The safety analysis in this study showed the overall incidence of TEAEs between Firsekibart and compound betamethasone group were comparable, and it remains consistent in the each eGFR subgroup analysis.

5. Conclusion

In summary, IL-1 β inhibitors have both theoretical and clinical research support for treating gout and reducing the progression of CKD. In this study, Firsekibart demonstrated non-inferior short-term pain relief while offering better prevention of new flares, with a lower incidence of serious adverse events compared to compound betamethasone, and results was consistent across eGFR subgroups. Both Firsekibart and compound betamethasone showed little effect on renal function.

This trial has several limitations. Firstly, it is a post-hoc subgroup analysis based on existing data, the sample size of each subgroup is small and the follow-up time is not long enough to confirm the observation of renal outcomes. Nevertheless, the results still provide a preliminary reference for clinical practice, and more researches with larger samples are needed to verify the above conclusions in the future.

Disclosure statement

The authors declare no conflict of interest.

References

- [1] Wang X, Luo D, Ru Y, et al., 2021, Guidelines for Hyperuricemia and Gout from the Perspective of Chronic Kidney Disease. *Chinese Journal of General Practice*, 24(33): 4191–4195.
- [2] Dehlin M, Jacobsson L, Roddy E, 2020, Global Epidemiology of Gout: Prevalence, Incidence, Treatment Patterns and Risk Factors. *Nature Reviews Rheumatology*, 16(7): 380–390.
- [3] Zhu Y, Pandya B, Choi H, 2012, Comorbidities of Gout and Hyperuricemia in the US General Population: NHANES

- 2007–2008. *American Journal of Medicine*, 125(7): 679–687.
- [4] Lee T, Chen J, Wu C, et al., 2021, Hyperuricemia and Progression of Chronic Kidney Disease: A Review from Physiology and Pathogenesis to the Role of Urate-Lowering Therapy. *Diagnostics*, 11(9): 1674.
 - [5] Xu D, Zhu X, Zou H, et al., 2023, Gout Diagnosis and Treatment Standards. *Chinese Journal of Internal Medicine*, 62(09): 1068–1076.
 - [6] Pofi R, Caratti G, Ray D, et al., 2023, Treating the Side Effects of Exogenous Glucocorticoids; Can We Separate the Good from the Bad? *Endocrine Reviews*, 44(6): 975–1011.
 - [7] Dumusc A, So A, 2015, Interleukin-1 as a Therapeutic Target in Gout. *Current Opinion in Rheumatology*, 27(2): 156–163.
 - [8] Loustau C, Rosine N, Forien M, et al., 2018, Effectiveness and Safety of Anakinra in Gout Patients with Stage 4–5 Chronic Kidney Disease or Kidney Transplantation: A Multicentre, Retrospective Study. *Joint Bone Spine*, 85(6): 755–760.
 - [9] Schlesinger N, Pillinger M, Simon L, et al., 2023, Interleukin-1 β Inhibitors for the Management of Acute Gout Flares: A Systematic Literature Review. *Arthritis Research & Therapy*, 25(1): 128.
 - [10] Schlesinger N, 2014, Anti-Interleukin-1 Therapy in the Management of Gout. *Current Rheumatology Reports*, 16(2): 398.
 - [11] Speer T, Dimmeler S, Schunk S, et al., 2022, Targeting Innate Immunity-Driven Inflammation in CKD and Cardiovascular Disease. *Nature Reviews Nephrology*, 18(12): 762–778.
 - [12] Liu Y, Lei H, Zhang W, et al., 2023, Pyroptosis in Renal Inflammation and Fibrosis: Current Knowledge and Clinical Significance. *Cell Death & Disease*, 14(7): 472.
 - [13] Xue Y, Chu T, Hu J, et al., 2025, Firsekibart in Acute Gouty Arthritis. *Journal of Translational Medicine*, 23(1): 91.
 - [14] Neogi T, Jansen T, Dalbeth N, et al., 2015, Gout Classification Criteria: An American College of Rheumatology/ European League Against Rheumatism Collaborative Initiative. *Annals of the Rheumatic Diseases*, 74(10): 1789–1798.
 - [15] Chapter 2: Definition, Identification, and Prediction of CKD Progression, 2013, *Kidney International Supplements*, 3(1): 63–72.
 - [16] Cipolletta E, Tata L, Nakafero G, et al., 2022, Association Between Gout Flare and Subsequent Cardiovascular Events Among Patients with Gout. *JAMA*, 328(5): 440–450.
 - [17] Bardin T, Nguyen Q, Tran K, et al., 2021, A Cross-Sectional Study of 502 Patients Found a Diffuse Hyperechoic Kidney Medulla Pattern in Patients with Severe Gout. *Kidney International*, 99(1): 218–226.
 - [18] Stamp L, Farquhar H, Pisaniello H, et al., 2021, Management of Gout in Chronic Kidney Disease: A G-CAN Consensus Statement on the Research Priorities. *Nature Reviews Rheumatology*, 17(10): 633–641.
 - [19] Im P, Kartsonaki C, Kakkoura M, et al., 2025, Hyperuricemia, Gout and the Associated Comorbidities in China: Findings from a Prospective Study of 0.5 million Adults. *Lancet Regional Health – Western Pacific*, 58: 101572.
 - [20] KDIGO, 2024, Clinical Practice Guideline for the Evaluation and Management of Chronic Kidney Disease. *Kidney International*, 105(4): S117–S314.
 - [21] Munar M, Singh H, 2007, Drug Dosing Adjustments in Patients with Chronic Kidney Disease. *American Family Physician*, 75(10): 1487–1496.
 - [22] Busso N, So A, 2010, Mechanisms of Inflammation in Gout. *Arthritis Research & Therapy*, 12(2): 206.
 - [23] Schreiber A, Pham C, Hu Y, et al., 2012, Neutrophil Serine Proteases Promote IL-1 β Generation and Injury in Necrotizing Crescentic Glomerulonephritis. *Journal of the American Society of Nephrology*, 23(3): 470–482.

- [24] Shi Y, 2010, Caught Red-Handed: Uric Acid is an Agent of Inflammation. *Journal of Clinical Investigation*, 120(6): 1809–1811.
- [25] Ponticelli C, Podesta M, Moroni G, 2020, Hyperuricemia as a Trigger of Immune Response in Hypertension and Chronic Kidney Disease. *Kidney International*, 98(5): 1149–1159.

Publisher's note

Bio-Byword Scientific Publishing remains neutral with regard to jurisdictional claims in published maps and institutional affiliations.

The Roles of E2F5 in Tumor Cell Cycle: The Gatekeeper or Destroyer?

Yingwen Du^{1,5†}, Danyun Wang^{1,5†}, Aidi Liang¹, Xinru Tang^{1,5}, Jiansen Chen^{1,5}, Ruizhi Yao^{1,2,3,4,5},

Lei Meng^{1,2,3,4,5}, Jianxing Xie^{1,2,3,4,5}, Ming Chen^{1,2,3,4,5}, Songtao Xiang^{1,2,3,4,5*}, Canbin Lin^{1,2,3,4,5*}

¹The First Affiliated Hospital of Guangzhou University of Chinese Medicine, Guangzhou, Guangdong, China

²Guangdong Clinical Research Academy of Chinese Medicine, Guangzhou, Guangdong, China

³Guangdong Engineering Research Center of Commercialization of Medical Institution Preparations and Traditional Chinese Medicines, Guangzhou, Guangdong, China

⁴Guangdong Engineering Technology Research Center of Commercialization of Lingnan Special Medical Institution Preparations, Guangzhou, Guangdong, China

⁵The First Clinical Medical School of Guangzhou University of Chinese Medicine, Guangzhou, Guangdong, China

† These authors contributed equally to this work and share the first authorship.

*Corresponding authors: Canbin Lin, lincb8818@163.com; Songtao Xiang, tonyxst@163.com

Copyright: © 2025 Author(s). This is an open-access article distributed under the terms of the Creative Commons Attribution License (CC BY 4.0), permitting distribution and reproduction in any medium, provided the original work is cited.

Abstract: E2F5 is a member of E2F transcription factor superfamily, controlling many molecular activities, such as cell proliferation, cell differentiation, DNA repair and cell death. Therefore, it is closely related to the occurrence, development and prognosis of a variety of cancers. In recent years, with the rapid development of bioinformatics, genomics and epigenetics, this study has further elucidated of E2F5 in the tumor cell cycle. Based on the latest research reports, this study reviewed the structural composition, dynamic activity regulation of E2F5, and how its transcription program driven by carcinogenic activity changed the progress of various tumor cell cycles, especially how it converted from a “gatekeeper” to a “destroyer”, thus affecting abnormal biological behaviors of tumor cells. Our aim is to provide a new direction for the development of E2F5 targeted therapy strategies and drug resistance in the future.

Keywords: E2F5; Retinoblastoma protein; Tumor cell cycle

Online publication: Oct 21, 2025

1. Introduction

In the early 1990s, Joe Nevins et al. found an active factor that induced the transcriptional activation of adenovirus E2 promoter at the early stage of replication, named as adenovirus early region 2 binding factor (E2F). They also found that adenovirus early region 1A (E1A) transforming protein could cause the reverse transcriptional activation of adenovirus E2 promoter, and stimulate the entry of cell cycle by inhibiting E1 related protein pRB and inducing the release of E2F agonist ^[1]. Subsequently, in 1995 Victoria buck screened another new member

of E2Fs family in a yeast two hybrid test. The homology of DNA binding domain with E2F4 was 87%, and the homology of tag box and pocket protein binding domain with the same region of E2F4 was respectively 75% and 72%, and the protein sequence and molecular tissue also had the same amino acid residues as E2F4. Based on this similarity, he named the new member E2F5, which represents a subfamily of E2F protein family with E2F4, and defined its molecular structure and physiological function for the first time ^[2].

Retinoblastoma protein (RB) plays the important role in regulating gene transcription and chromatin remodeling, affecting cell cycle progression, cell senescence and tumorigenesis. As the first tumor suppressor discovered, RB is absent or mutated in at least one third of human tumors. Rb-E2F pathway integrates proliferation signals with cell cycle checkpoints to ensure proper cell division and genomic integrity ^[3]. The precise regulation of E2F activity makes RB plays a central role in determining cell fate.

Cancer is a polygenic disease in the eukaryotic cell cycle, involving the genetic and epigenetic changes of key genes in the cell cycle. The cell cycle is a series of highly organized events. Multiple checkpoints have been set up to monitor the growth signal and DNA integrity during cell proliferation. Among them, G₁/S phase transition is crucial to maintain DNA conservation. The CDK-RB-E2F axis is the core transcription mechanism driving the cell cycle process, determining the spatiotemporal nature of genome replication and the accuracy of genetic material transmission. As the final effector, E2F transcription factor family is encoded by eight genes into transcriptional activators and transcriptional inhibitors, which are involved in many important cellular processes, such as cell proliferation, differentiation and apoptosis. As one of the classic E2F family inhibitors, the expression of E2F5 is cell cycle dependent and mainly regulates gene expression in G₁ and S phases, just like the gatekeeper standing in front of the checkpoint. Abnormal expression and activity of E2F5 may lead to malignant cell proliferation, which is a common phenomenon in various cancers.

Therefore, this article describes the structural composition of E2F5 and its dynamic activity regulation in the cell cycle, focusing on how its transcription program driven by carcinogenic activity changes the progress of tumor cell cycle, converted from the gatekeeper to the destroyer, then affects the abnormal biological behavior of tumor cells such as proliferation, migration, invasion and apoptosis.

2. E2F5 molecular structure

In cytogenetics, E2F5 gene is located on human chromosome 8q21.2 and contains 10 exons. It is encoded by 346 amino acids and has a predicted molecular weight of 38 kDa. E2F5 contains three highly conserved active regions: the wing helix DNA binding domain, the dimer domain, and the reverse transcription activation domain. The E2F family recognizes TTT (C/G) (C/G) (C/G) CGC, a consistent DNA sequence in the promoter of target genes. The E2F5 dimer domain consists of a heterodimer helix Helicon domain and a heterodimer β - sandwich domain connected by two small helices and two small chains. Before binding to DNA, E2F5 needs to interact with transcription factor dimers (TFDP1, TFDP2 and TFDP3) to form a dimer through protein-protein interaction through oligomerization sites on the dimer domain, containing leucine zipper (LZ) and marker frame (MB) domains ^[1,4]. The amino acid sequence at the oligomerization site has strong conservation, and connecting with the DNA binding domain and forms a certain spatial conformation. It is reported that TFDP1 and TFDP2 can be identified in humans, mice, dogs and other species, while TFDP3 is not found in mouse cells, but can be captured in humans and highly expressed in many malignant tumors ^[5]. Although TFDP3 has high sequence homology with TFDP1 and TFDP2, and combining with E2F family members to enhance E2F DNA binding activity. However,

TFDP3 can down regulate E2F family mediated transcriptional activation. Most E2Fs and TFDP1/2 are mainly nuclear localization, While the subcellular localization of TFDP3 is cell cycle specific. It is expressed in the nucleus of G₁ phase and the end of mitosis, and in the cytoplasm of S phase and G₂ phase, which is similar to the cell cycle specific localization of E2F4 and E2F5. In quiescent cells (G₀), the inhibited E2F5 mainly interacts with TFDP1/2 to block the transcription of cell cycle related genes. In circulating cells, E2F5 and TFDP1/2/3 are shuttled into the cytoplasm after the pocket protein in the middle and late stages of G₁ is phosphorylated and inactivated. At the same time, E2F1-3 combines with TFDP1/2 to activate target gene transcription, promote G₁–S phase transition, or form a complex with TFDP3 to inhibit its activity level, resulting in E2F activity threshold not reaching the limit point of G₁–S phase transition, and cell cycle is blocked in G₁ phase^[6].

When E2F and DP protein family members interact as E2F/DP heterodimers, E2F has physiological functions and its transcriptional activity is regulated by the physical association of different pocket protein family members. The members of pocket protein family are composed of N-terminal domain, pocket domain and disordered sequence, including C-terminal domain, inter domain linker and pocket ring. The pocket domain is divided into two non-covalently interacting subdomains composed of folded cyclins and three additional helices. It is combined with E2F reverse transcription activation domain through LxCxE. The C-terminal domain not only forms another binding plane with the marker frame domain of E2F/DP heterodimer, but also contains the docking sites of a variety of kinases and phosphatases. It is reported that the deficiency of LXCXE binding function of RB will lead to the significant increase of E2F3 level and promote tumorigenesis, and the deletion of LXCXE binding domain will also lead to the instability of mouse genome, emphasizing that RB plays an important role in maintaining the stability of chromosome structure^[7,8].

Different pocket protein subtypes (RB, p107 and p130) are different from each other. For example, p107 and p130 have 54% sequence homology, 30% homology with RB and similar domain structure^[9]. Both pocket proteins can bind to E2F5, but p107 and p130 almost only bind specifically to E2F4 and E2F5. Tyler J. Liban et al. discovered that the C-terminal domain of p107 has a higher affinity for E2F4/5 by using structural and biochemical analysis, which is necessary to mediate the growth inhibition function, and p107 is only related to E2F4/5^[3].

Unlike E2F1-3, E2F4 and E2F5 do not have inherent nuclear localization signals (NLS), but contain nuclear export signals (NES). The nuclear localization signal activity is provided by DP heterodimer chaperone or pocket protein trans. The nuclear cytoplasmic localization of E2F5 in the cell cycle is consistent with the expression fluctuation of pocket protein in regulating nuclear accumulation, indicating that the nuclear cytoplasmic shuttle activity mediated by E2F nuclear accumulation mechanism plays a significant role in the cell cycle^[10].

3. Role of E2F5 in cell cycle

Cell cycle refers to the process from the end of parental cell division to the end of offspring cell division. It is composed of G₁, S, G₂ and M phases, among which G₁, S and G₂ phases are collectively referred to as interphase. Mammalian cells are highly controlled by both positive and negative growth regulatory signals in the G₁/S phase. By regulating the transcriptional activation of E2F, the cells make irreversible DNA replication. Accordingly, E2F is crucial in the proliferation control of normal cells and tumor cells.

A single subtype of E2F will show different expression levels and activity patterns throughout the cell cycle. The nature of cell cycle dependent dynamic gene expression is driven by the sequential combination of E2F activators and inhibitors with target promoters, requiring the coordination of gene expression and cell cycle

regulatory proteins. One of the key periods is the transition from G₁ phase to S phase, and E2F5, RB and other afferent regulatory factors play a pivotal role in this transition process. They are strictly regulated in transcription, mRNA stability, post-translational modification, protein-protein interaction and protein stability. Here this study summarizes the main regulatory mechanisms of E2F5 in the cell cycle.

3.1. Pocket protein regulates E2F5 by phosphorylation

Pocket protein family is a critical negative regulator of cell cycle, regulating transcription by directly inhibiting E2F and recruiting transcriptional co regulators that modifying histone and chromatin structures. In G₀ phase, dephosphorylated pocket protein combines with E2F5 reverse transcription activation domain to form inhibition complex with a variety of cofactors on the target gene promoter, directly inhibiting the expression of target gene. In G₁ phase, when mitogen activated protein kinase signaling pathway transmits extracellular signals through kinase cascade reaction, it triggers cell proliferation, forms a complex between cyclin and cyclin dependent kinase (CDK), phosphorylates serine 807/811 (S807/811) and threonine 821 (T821) sites of RB, and turns RB into pRB. After RB inactivation, E2F5 is released from the complex and shuttles to the cytoplasm, increasing E2F activator activity and inducing transcriptional activation of G₁-S phase target genes, promoting the process of cell cycle. RB plays a major role in protecting genomic integrity and preventing uncontrolled cell proliferation, and is a key barrier to prevent tumorigenesis.

RB is an important barrier to prevent tumorigenesis, plays the crucial role in protecting genome integrity and preventing uncontrolled cell proliferation. RB knockout is fatal in mouse embryos, and knockout of p107 or p130 will lead to a viable phenotype^[11,12]. In addition, the tumor suppressive characteristics of RB gene are considered to be stronger than p107 and p130, and mutations are often found in human tumor cells^[13,14]. In contrast, p107 and p130 gene mutations are not common in cancer. Heterozygous mutant RB mice spontaneously develop tumors, while p107 and p130 mutant mice do not. Many tumorigenesis and pathological states are related to the loss of control caused by cell cycle checkpoint interruption. For example, overexpression of RB inhibits early events in G₁ phase and prevents cells from entering S phase. Then RB gradually phosphorylates from G₁ phase to G₂ phase, completing the complete closed loop of positive and negative regulatory signaling pathways in cell cycle. The accumulation of RB in the cytoplasm is significantly related to the phosphorylation of serine 795 (S795) site, resulting in the weakening of its tumor inhibitory activity in the nucleus^[15].

On the one hand, RB combined with E2F5 to block the transcription of target genes, showing the ability of “inhibit activation”. On the other hand, RB-E2F5 complex retains the ability to bind to the promoter of the target gene, and recruits’ factors, such as histone deacetylases (HDACs) and methyltransferases, that affect the gene and chromatin structure, resulting in transcriptional inhibition, showing the ability of “active inhibition”. Loss of RB function or dysfunction of related pathways can lead to excessive cell proliferation, genomic instability and accumulation of gene mutations. Furthermore, RB signaling pathway is intertwined with other signaling cascades involved in cell cycle regulation and tumor inhibition, such as MARK, p53, PI3K-Akt-mTOR, increasing the complexity of cell cycle regulation.

In summary, the imbalance of RB-E2F5 signal will destroy the intracellular homeostasis. Whether it is gene mutation, functional defect, epigenetic change or environmental induction, it can release the carcinogenic potential of cells, leading to the occurrence, development and treatment resistance of tumors. On the contrary, changes in the expression or activity of Rb and E2F5 may lead to sensitivity or resistance to specific anti-tumor therapy, making them potential predictive markers of tumor therapy.

3.2. Regulation of subcellular localization on E2F5

Most of E2Fs were mainly located in nucleus, but E2F5 showed cell cycle specific localization. The nuclear export signal of E2F5 is mediated by a transporter protein (XPO1, also known as CRM1), which is located in the nucleus of quiescent cells and in the cytoplasm of circulating cells. Allen et al. found that the nuclear localization signal accumulation of E2F5 is produced by DP or supplied by physically related pocket protein trans. On the one hand, the cytoplasmic localization of E2F5 may be passive, and E2F5 combined with DP can overcome the interaction with nuclear localization signals. DP plays a dominant role in regulating nuclear localization signal in DP/E2F5. On the other hand, when E2F5 was co-expressed with DP-1 and p107, p107 significantly changed the nuclear localization ratio of DP/E2F5 (from $\leq 5\%$ to $> 90\%$), indicating that pocket protein trans provided nuclear localization to control the nuclear accumulation of DP/E2F5. It is worth noting that the nuclear accumulation of E2F5/DP is regulated by cell cycle. When E2F5 and DP-3 coexist, the proportion of cells in G₂/M phase will increase significantly. In contrast, under the same conditions, the co-expression of E2F5 and p107 lead to the accumulation of G₁ phase, and E2F5 is co-expressed with DP-3/p107 in the nucleus. Different E2F5 nuclear accumulation mechanisms have different biological consequences on cell cycle progression. When mediated by DP chaperone, cells receive stimulation to promote growth. While mediated by pocket protein, cell cycle progression is blocked, thus maintaining the transcriptional activity of E2F target gene^[16].

3.3. Self-transcription and post transcriptional regulation of E2F5

In terms of self-transcription, E2F5 completes a cell cycle through self-regulation. in the early stage of G₁, E2F5 was released from the inhibition of pocket protein, to combine with pocket protein and return to the nucleus in the late stage of mitosis, formed a closed loop. At the post transcriptional level, E2F5 mRNA stability and translation are strictly regulated by a variety of miRNAs. For example, miR-154 is reported to be abnormally expressed in prostate cancer, hepatocellular carcinoma and renal cell carcinoma^[17–19]. The former two are used as tumor suppressors to inhibit growth and proliferation, while in renal cell carcinoma, mir-154 is used as a carcinogen to participate in cancer cell proliferation and anti-apoptosis. Moreover, targeted miRNA has a profound impact on tumor drug resistance. Such as miRNA-34a targeted down regulated E2F5 expression, significantly enhancing the sensitivity of gastric cancer cells to paclitaxel treatment and overexpression of mir-544 in esophageal squamous cell carcinoma targets E2F5 to enhance cisplatin sensitivity^[20,21]. Multiple miRNAs can adjust the expression and activity of E2F5, thereby regulating a variety of E2F5 target genes and affecting biological processes related to cell proliferation. On the contrary, E2F5 can regulate the expression of multiple miRNAs to build an interactive regulatory network.

4. Role of E2F5 in tumor cells

Malignant tumors produce drug resistance by changing the cell cycle process which also known as cell cycle specific mechanism or upstream signaling pathway which also known as cell cycle nonspecific mechanism and the imbalance of cell proliferation and apoptosis signal regulation is related to tumorigenesis. As a member of the core cell cycle mechanism, E2F5 is involved in the occurrence and development of a variety of cancers.

4.1 Renal cell carcinoma (RCC)

The expression level of E2F5 in clear cell renal cell carcinoma (ccRCC) decreased, and its low expression was significantly correlated with longer overall survival, disease-specific survival and progression free survival. It

was also an independent factor related to overall survival and progression free survival in patients with ccRCC, and its expression was significantly correlated with DNAmethylation and copy number^[51]. E2F5 also showed a low expression level in chromophobe renal cell carcinoma (chRCC), and the expression level was correlated with the histological grade of chRCC, including T and N stages^[52].

4.2. Ovarian cancer

E2F5 is overexpressed in the early stage of ovarian cancer, especially in serous and endometrioid ovarian cancer. The expression of E2F5 can be up-regulated to 5 times in the process of early progression to advanced stage, so it is considered to be a carcinogen. When E2F5 and CA125 are combined, the sensitivity and specificity of detection of epithelial ovarian cancer (EOC) can be improved to 97.9% and 72.5%^[22,23]. Daniel et al. found that the response of different E2F to INF- γ intervention is heterogeneous, and the increased expression of E2F5 is the key factor for INF- γ to play an anti-proliferative role in ovarian cancer cells^[24]. In recent years, E2F5 has been found to be highly expressed in cisplatin resistant ovarian cancer cells and promotes proliferation as a positive regulator, indicating that E2F5 may be a new target for the treatment of drug-resistant ovarian cancer. Knockdown of E2F5 can reduce the expression levels of cyclin D1, CDK4 and pRB through *Hippo* and *Wnt- β -Catenin* pathways, make cells accumulate in G₀/G₁ phase, and significantly block the cell cycle from entering G₁/S phase^[25-27]. FAT4 can reduce the expression of E2F5, promote the transition of G₁/S phase of cell cycle, and accelerate cell growth and epithelial-mesenchymal transition^[26].

4.3. Breast cancer

E2F5 specific signal is located between MOS (8q12) and MYC (8q24), which is also the place where 50–60% of breast cancer genes are amplified, indicating that E2F5 may cooperate with other oncogenes to promote cell transformation and thus promote the occurrence and development of tumors^[28]. It is reported that the abnormal methylation degree of E2F5 in breast cancer tissues is low, and its promoter methylation frequency is also low, and the methylation degree of well differentiated tumors is often lower than that of poorly differentiated tumors^[29]. Carson broeker et al. detected that E2F5 deficient mice retained the integrity of lactation function, but also spontaneously developed into highly metastatic breast cancer after a long incubation period^[29].

In triple negative breast cancer (TNBC), overexpression of E2F5 was more common, and increased E2F5 was also observed in tissues with high Ki-67. In addition, the positive expression of E2F5 in patients with negative lymph nodes will show worse clinical prognosis and shorter disease-free survival. The overexpression of E2F5 is associated with invasive histopathology and worse clinical prognosis^[30]. Down regulation of E2F5 could reduce the proliferation rate of tumor cells and induce the death of ER⁽⁺⁾ breast cancer cells with wild-type TP53, but had little effect on TNBC cells with TP53 mutation and Her-2⁽⁺⁾ breast cancer cells. Although there was a slight increase in G₂/M phase cells in E2F5 deleted TNBC cells, the fluctuation of p21WAF1 expression was not found after E2F5 deletion in TNBC cells, and there was no increase in G₂/M phase cells in HER-2⁽⁺⁾ breast cancer cells^[31].

4.4. Hepatocellular carcinoma

The increased expression of E2F5 in hepatocellular carcinoma (HCC) tissues is significantly correlated with tumor stage and poor overall survival^[32]. Ji et al. described that FOXN3 inhibits E2F5 expression by directly combining with its promoter, but this inhibition can be reversed by up regulating E2F5^[33]. Contrary to the above conclusion, Zou et al. found that the expression of E2F5 was down regulated in HBV infection related HCC cells, and the level of HBV infection was negatively correlated with the expression of E2F5, revealing that the cell growth promoting

mechanism of HBV may play an important role in the progress of HBV related HCC ^[34]. Jiang et al. identified that the 8q21.2 locus, also the E2F5 locus gene of primary HCC was repeatedly amplified through genome-wide, microarray, and comparative genomic hybridization analysis. Down regulation of E2F5 could significantly inhibit the growth of HCC cells and block the cell cycle at G₀/G₁ phase. E2F5 may be involved in the regulation of early G₁ events, including G₀/G₁ phase transition, lifting the restriction of checkpoints, inducing uncontrollable cell cycle progression in hepatocytes, and ultimately promoting cancer transformation through joint action with other carcinogens ^[35].

4.5. Prostatic cancer

E2F5 is a carcinogen gene in prostatic cancer (PCa). Overexpression of E2F5 was significantly correlated with high Gleason score, high transcription level, high biochemical recurrence risk, advanced tumor stage, metastasis and low survival rate after metastasis. E2F5 low expression tissues are often accompanied by abundant plasma cells and NK cells, driving antibody-dependent cell-mediated cytotoxicity (ADCC) to promote anti-tumor immunity. E2F5 may potentially affect the progress of PCA by interfering with anti-tumor immunity ^[36]. Increased copy numbers of E2F5 and MYC were also observed in the chromosome 8q21-24 region of PCa cells, and their synergistic effect may be related to invasive clinicopathological features ^[37]. Qi et al. discovered that endogenous CDK13 can promote the formation of circ-CDK13 and significantly promote the expression of E2F5 by reducing the expression of miR-212-5p/449. As a transcription activator of CDK13, E2F5 also stimulates the transcription of CDK13. This positive feedback regulation promotes the growth and proliferation of PCa cells, and this circ-RNA produced with the transcription of primary genes regulates the expression of primary genes and downstream target genes through positive feedback, which may be one of the important reasons for the drug resistance of tumor cells to molecular targeted drugs ^[38].

It is reported that E2F5 may be involved in the regulation of G₀/G₁ phase of PCa cells. Majumder s et al. found that the transcription level of E2F5 in tumor tissues with Gleason score of 6 was significantly higher than that in tumor tissues and benign prostatic hyperplasia (BPH) tissues with Gleason score greater than 6. They further verified that E2F5 and SMAD3 were co-located in PCa cells, and their distribution in the nucleus was increased. Down regulation of E2F5 would reduce the phosphorylation level of p38 and SMAD3, leading to the arrest of PCa cells in G₁ phase ^[39]. Li et al. reported that overexpression of E2F5 and (or) PFTK1 was significantly associated with the highly invasive PCa phenotype. Silencing E2F5 and PFTK1 not only significantly increased the proportion of G₀/G₁ phase cells, but also inhibited the expression of CDK2 and CDK4 ^[40]. Tariq a. bhat et al. clarified that decursin downregulated ERK1/2 phosphorylation by targeting EGFR-ERK1/2 pathway, increased the expression of p27, p107 and p130, but significantly reduced the expression levels of E2F5, CDK2 and CDK4, thereby inducing strong G₁ arrest and cell death of PCa cell ^[41]. Karmakar deepmala et al. showed that E2F5 as a bifunctional transcription factor, on the one hand inhibited the expression of TFPI2 (TFPI2 negatively regulated the level and activity of MMP-2 and MMP-9), on the other hand activated the transcriptional expression of MMP-2 and MMP-9 genes. They also found that artemisinin can reduce the expression of E2F5 and reverse the dysfunctional interaction between TFPI2 and MMPs in PC3 cells ^[42]. It has been reported that artemisinin can trigger G₁ phase arrest and improve the proliferation rate and invasiveness of PCa cells ^[43]. However, the relevant mechanism of artemisinin mediated E2F5 down-regulation remains to be explored. Similarly, Chapla Agarwal

et al. observed that IP6 could significantly reduce E2F5 protein levels by 70% with the increase of dose and the extension of treatment time, and reduce the molecular levels of CDK4, cyclin D1, pRB and other molecules involved in the control of G₁/S phase transition. Besides, IP6 also induced the expression of Cip1/p21 and Kip1/p27, resulting in the decrease of Bcl-2 and the increase of Bax/Bcl-2 ratio, and the strong accumulation of cell cycle in G₁ phase accompanied by the decrease of S phase and G₂/M phase ^[44]. According to the report, cell apoptosis often occurs in G₁ phase, and G₁/S phase arrest can accelerate cell apoptosis, suggesting that IP6 may simultaneously activate cell proliferation arrest and apoptosis to induce the growth inhibition of PCa cells ^[45].

4.6. Other malignant tumors

In head and neck squamous cell carcinoma (HNSCC), gastric cancer, colon cancer and esophageal squamous cell carcinoma (ESCC), E2F5 overexpression was found, and was significantly correlated with pathological malignancy, poor prognosis and low overall survival. It was also negatively correlated with the infiltration of activated dendritic cells, macrophages, neutrophils and NK cells ^[46–50]. At present, the “protective” characteristics of E2F5 in renal cell carcinoma are still unexplained, which may be related to cell proliferation, differentiation, DNA repair, cell cycle control and cell death, and the related mechanism remains to be further studied.

The stable expression of E2F5 can specifically induce quiescent cells to enter the cell cycle, and its abnormal expression behavior may be determined by the specific cell environment, the existence of overlapping binding sites and the interaction between promoter and target genes. In a study on cervical cancer associated with high-risk human papillomavirus (HPV) infection, HPV 18 converts E2F5 into an activator by directly transcribing and activating the major carcinogenic protein E7. E2F5 directly activates E6/E7 transcription, overcomes G₀/G₁ checkpoint blocking by degrading p53 and pRB, and indirectly and positively regulates the entry of cells into S phase. The transition of E2F5 from inhibition to activation may enhance the carcinogenic potential of HPV18 and promote the progression of cervical cancer ^[53]. Down regulation of E2F5 in pancreatic cancer and neuroblastoma can trigger G₀/G₁ phase block. Knockout of E2F5 in gastric cancer can increase the number of cells in G₁ phase and reduce the number of cells in S phase, leading to the stagnation of tumor cells in G₁/S phase ^[54–56]. In general, E2F5 seems to act as a gatekeeper to control the transcription and expression of target genes at immune checkpoints during early cell cycle events, especially the transition from quiescent cells to circulating cells. Its precise regulation of cell cycle is an important guarantee to ensure growth, proliferation and differentiation. The abnormal expression of E2F5 is common in various tumors, and it seems that the transition from the “gatekeeper” to the “destroyer” has made it the latest breakthrough point in current cancer treatment.

5. Conclusion and perspective

The abnormal activity of core cell cycle mechanism basically exists in all tumor types, and it is also the driving force of tumor occurrence and progression. E2F5, as one of the core gatekeepers of cell cycle, mainly regulates the gene expression in G₁/S phase, showing the characteristics of cell cycle dependence. Its precise expression and activity are crucial for protecting cells from abnormal proliferation, ensuring the spatiotemporal nature of genome replication and the accuracy of genetic material transfer. However, the abnormal expression and activity of E2F5 are also important mechanisms for the occurrence and development of various cancers. Cancer cells with uncontrolled proliferation use the characteristics of E2F5 in different ways, strengthening the uniqueness and dependence of E2F5 program driven by oncogenes. The abnormal expression of E2F5 in tumor cells may be a manifestation of tumor specificity. More and more evidences show that the change of E2F5 expression is the key

mechanism of chemotherapy resistance of cancer cells, especially in the presence of CDK4/6 inhibitors. Therefore, E2F5 is a potential biomarker for molecular diagnosis.

Funding

National Natural Science Foundation of China (Project No.: 82205126); Scientific Research Project of Guangdong Provincial Administration of Traditional Chinese Medicine (Project No.: 20251104); Guangdong Famous Traditional Chinese Medicine Studio, 4th Batch of Famous Traditional Chinese Medicine Master-Apprentice Program in Guangdong Province in 2024 (Jianxing Xie); Young and Middle-aged Key Talent Training Project of The First Affiliated Hospital of Guangzhou University of Chinese Medicine (Project No.: 09005650043)

Disclosure statement

The authors declare no conflict of interest.

References

- [1] Trimarchi J, Lees J, 2002, Sibling Rivalry in the E2F Family. *Nature Reviews Molecular Cell Biology*, 3: 11–20.
- [2] Buck V, Allen K, Sørensen T, et al., 1995, Molecular and Functional Characterisation of E2F-5, a New Member of the E2F Family. *Oncogene*, 11(1): 31–38.
- [3] Liban T, Medina E, Tripathi S, et al., 2017, Conservation and Divergence Of C-Terminal Domain Structure in the Retinoblastoma Protein Family. *Proceedings of the National Academy of Sciences of The United States of America*, 114: 4942–4947.
- [4] Rubin S, Gall A, Zheng N, et al., 2005, Structure of the Rb C-Terminal Domain Bound to E2F1-DP1: A Mechanism for Phosphorylation-Induced E2F Release. *Cell*, 123(6): 1093–1106.
- [5] Qiao H, Di Stefano L, Tian C, et al., 2007, Human TFDP3, A Novel DP Protein, Inhibits DNA Binding and Transactivation by E2F. *Journal of Biological Chemistry*, 282(1): 454–466.
- [6] Huang J, Wang Y, Liu J, et al., 2021, TFDP3 As E2F Unique Partner, Has Crucial Roles in Cancer Cells and Testis. *Frontiers In Oncology*, 11: 742462.
- [7] Ryan J, Bourgo R, Chellappagounder T, et al., 2011, RB Restricts DNA Damage-Initiated Tumorigenesis Through An LXCXE-Dependent Mechanism of Transcriptional Control. *Molecular Cell*, 43(5): 663–672.
- [8] Courtney H, Coschi A, Martens K, et al., 2010, Mitotic Chromosome Condensation Mediated by the Retinoblastoma Protein Is Tumor-Suppressive. *Genes & Development*, 24(13): 1351–1363.
- [9] Liban T, Thwaites M, Dick F, et al., 2016, Structural Conservation and E2F Binding Specificity Within the Retinoblastoma Pocket Protein Family. *Journal Of Molecular Biology*, 428(19): 3960–3972.
- [10] Krek W, Ewen M, Shirodkar S, et al., 1998, Distinct Mechanisms of Nuclear Accumulation Regulate the Functional Consequence of E2F Transcription Factors. *Journal of Cell Science*, 111: 2819–2831.
- [11] Jacks T, Fazeli A, Schmitt E, et al., 1992, Effects of an Rb Mutation in The Mouse. *Nature*, 359(6397): 295–300.
- [12] Lee M, Williams B, Mulligan G, et al., 1996, Targeted Disruption Of p107: Functional Overlap Between p107 And Rb. *Genes & Development*, 10(13): 1621–1632.
- [13] Dick F, Rubin S, 2013, Molecular Mechanisms Underlying RB Protein Function. *Nature Reviews Molecular Cell*

Biology, 14(5): 297–306.

- [14] Classon M, Harlow E, 2002, The Retinoblastoma Tumour Suppressor in Development and Cancer. *Nature Reviews Cancer*, 2(12): 910–917.
- [15] Burke J, Hura G, Rubin S, 2012, Structures of Inactive Retinoblastoma Protein Reveal Multiple Mechanisms for Cell Cycle Control. *Genes & Development*, 26(11): 1156–1166.
- [16] De La Luna S, Burden M, Lee C, et al., 1998, Nuclear Accumulation of E2F-4 Is Regulated by Protein Stability and Protein Phosphatase 1 Activity in a Cell Cycle-Dependent Manner. *Journal Of Cell Science*, 111(17): 2605–2616.
- [17] Chen Z, Pengfei S, Meiling B, et al., 2014, miR-154 Inhibits Prostate Cancer Cell Proliferation by Targeting CCND2. *Urologic Oncology: Seminars And Original Investigations*, 32(1): 31.e9–31.e16.
- [18] Lin C, Li Z, Chen P, et al., 2018, Oncogene miR-154-5p Regulates Cellular Function and Acts as a Molecular Marker with Poor Prognosis in Renal Cell Carcinoma. *Life Sciences*, 209: 289–297.
- [19] Pang X, Huang K, Zhang Q, et al., 2015, miR-154 Targeting ZEB2 In Hepatocellular Carcinoma Functions as a Potential Tumor Suppressor. *Oncology Reports*, 34(6): 3273–3280.
- [20] Li L, Wu C, Zhao Y, 2017, miRNA-34a Enhances the Sensitivity of Gastric Cancer Cells to Treatment with Paclitaxel by Targeting E2F5. *Oncology Letters*, 13(1): 63–68.
- [21] Sun F, Zhang C, Ma D, et al., 2019, MicroRNA-544 Inhibits Esophageal Squamous Cell Carcinoma Cell Proliferation and Enhances Sensitivity to Cisplatin by Repressing E2F Transcription Factor 5. *Oncology Letters*, 18(3): 2553–2561.
- [22] Collins Y, Tan D, Pejovic T, et al., 2004, Identification of Differentially Expressed Genes in Clinically Distinct Groups of Serous Ovarian Carcinomas Using cDNA Microarray. *International Journal of Molecular Medicine*, 14(2): 281–287.
- [23] Kothandaraman N, Bajic V, Brendan P, et al., 2010, E2F5 Status Significantly Improves Malignancy Diagnosis of Epithelial Ovarian Cancer. *BMC Cancer*, 10: 64.
- [24] Reimer D, Sadr S, Wiedemair A, et al., 2006, Heterogeneous Cross-Talk of E2F Family Members Is Crucially Involved in Growth Modulatory Effects of Interferon-Gamma and EGF. *Cancer Biology & Therapy*, 5(10): 1405–1412.
- [25] Wang Y, Wang X, Han L, et al., 2020, LncRNA MALAT1 Regulates the Progression and Cisplatin Resistance of Ovarian Cancer Cells via Modulating miR-1271-5p/E2F5 Axis. *Cancer Management and Research*, 12: 9999–10009.
- [26] Malgundkar S, Burney I, Al-Moundhri M, et al., 2020, FAT4 Silencing Promotes Epithelial-To-Mesenchymal Transition and Invasion Via Regulation of YAP and β -Catenin Activity in Ovarian Cancer. *BMC Cancer*, 20(1): 374.
- [27] Malgundkar S, Burney I, Al-Moundhri M, et al., 2021, E2F5 Promotes the Malignancy of Ovarian Cancer via the Regulation of Hippo and Wnt Pathways. *Genetic Testing and Molecular Biomarkers*, 25(4): 255–264.
- [28] Polanowska J, Le Cam L, Orsetti B, et al., 2000, Human E2F5 Gene is Oncogenic in Primary Rodent Cells and is Amplified in Human Breast Tumors. *Genes Chromosomes Cancer*, 28: 126–130.
- [29] Umemura M, Shirane S, Takekoshi S, et al., 2009, Overexpression of E2F-5 Correlates with a Pathological Basal Phenotype and a Worse Clinical Outcome. *British Journal of Cancer*, 100(5): 764–771.
- [30] To B, Broecker C, Jhan J, et al., 2024, Insight into Mammary Gland Development and Tumor Progression in an E2F5 Conditional Knockout Mouse Model. *Oncogene*, 43(12): 876–889.
- [31] Inagaki Y, Wu D, Fujiwara K, et al., 2020, Knockdown of E2F5 Induces Cell Death Via the TP53-Dependent Pathway in Breast Cancer Cells Carrying Wild-Type TP53. *Oncology Reports*, 44(5): 2023–2032.
- [32] Kim T, Yim S, Shin S, et al., 2008, Clinical Implication of Recurrent Copy Number Alterations in Hepatocellular

- Carcinoma and Putative Oncogenes in Recurrent Gains On 1q. *International Journal of Cancer*, 123(12): 2808–2815.
- [33] Sun J, Li H, Huo Q, et al., 2016, The Transcription Factor FOXN3 Inhibits Cell Proliferation by Downregulating E2F5 Expression in Hepatocellular Carcinoma Cells. *Oncotarget*, 7(28): 43534–43545.
- [34] Zou C, Li Y, Cao Y, et al., 2014, Up-Regulated MicroRNA-181a Induces Carcinogenesis in Hepatitis B Virus-Related Hepatocellular Carcinoma by Targeting E2F5. *BMC Cancer*, 14: 97.
- [35] Jiang Y, Yim S, Xu H, et al., 2011, A Potential Oncogenic Role of the Commonly Observed E2F5 Overexpression in Hepatocellular Carcinoma. *World Journal of Gastroenterology*, 17(4): 470–477.
- [36] Han Z, Mo R, Cai S, et al., 2022, Differential Expression of E2F Transcription Factors and their Functional and Prognostic Roles in Human Prostate Cancer. *Frontiers In Cell and Developmental Biology*, 10: 828659.
- [37] Zhao J, Wu X, Ling X, et al., 2013, Analysis of Genetic Aberrations on Chromosomal Region 8q21–24 Identifies E2F5 as an Oncogene with Copy Number Gain in Prostate Cancer. *Medical Oncology*, 30: 1–10.
- [38] Qi J, Yang Z, Lin T, et al., 2021, CDK13 Upregulation-Induced Formation of the Positive Feedback Loop Among circCDK13, miR-212-5p/miR-449a And E2F5 Contributes to Prostate Carcinogenesis. *Journal Of Experimental & Clinical Cancer Research*, 40: 1–18.
- [39] Majumder S, Bhowal A, Basu S, et al., 2016, Deregulated E2F5/p38/SMAD3 Circuitry Reinforces the Pro-Tumorigenic Switch of TGF β Signaling in Prostate Cancer. *Journal of Cellular Physiology*, 231(11): 2482–2492.
- [40] Sen-Mao L, Huan-Lei W, Xiao Y, et al., 2018, The Putative Tumour Suppressor miR-1-3p Modulates Prostate Cancer Cell Aggressiveness by Repressing E2F5 And PFTK1. *Journal Of Experimental & Clinical Cancer Research*, 37(1): 169.
- [41] Bhat T, Dheeraj A, Nambiar D, et al., 2023, Decursin Inhibits EGFR-ERK1/2 Signaling Axis in Advanced Human Prostate Carcinoma Cells. *The Prostate*, 83(16): 1551–1567.
- [42] Karmakar D, Maity J, Mondal P, et al., 2020, E2F5 Promotes Prostate Cancer Cell Migration and Invasion Through Regulation of TFPI2, MMP-2 And MMP-9. *Carcinogenesis*, 41: 1767–1780.
- [43] Efferth T, Dunstan H, Sauerbrey A, et al., 2001, The Anti-Malarial Artesunate Is Also Active Against Cancer. *International Journal of Oncology*, 18: 767–773.
- [44] Agarwal C, Dhanalakshmi S, Singh R, et al., 2004, Inositol Hexaphosphate Inhibits Growth and Induces G1 Arrest and Apoptotic Death of Androgen-Dependent Human Prostate Carcinoma LNCaP Cells. *Neoplasia*, 6: 646–659.
- [45] Craig C, Wersto R, Kim M, et al., 1997, A Recombinant Adenovirus Expressing p27Kip1 Induces Cell Cycle Arrest and Loss of Cyclin-Cdk Activity in Human Breast Cancer Cells. *Oncogene*, 14(19): 2283–2289.
- [46] Li Y, Huang Y, Li B, et al., 2023, Roles of E2F family members in the diagnosis and prognosis of head and neck squamous cell carcinoma. *BMC medical genomics*, 16(1), 38.
- [47] Li S, Yang X, Li W, et al., 2021, Comprehensive Analysis of E2F Family Members in Human Gastric Cancer. *Frontiers In Oncology*, 11: 633960.
- [48] Yao H, Lu F, Shao Y, 2020, The E2F Family as Potential Biomarkers and Therapeutic Targets in Colon Cancer. *PeerJ*, 8: e8562.
- [49] Takeshi I, Atsushi S, Daisuke I, et al., 2013, E2F5 As an Independent Prognostic Factor in Esophageal Squamous Cell Carcinoma. *Anticancer Research*, 33(12): 5415–5422.
- [50] Gan Z, Abudurexiti A, Hu X, et al., 2024. E2F3/5/8 serve as potential prognostic biomarkers and new therapeutic direction for human bladder cancer. *Medicine*, 103(2), e35722.
- [51] Liu Z G, Su J, Liu H, et al., 2022. Comprehensive bioinformatics analysis of the E2F family in human clear cell renal cell carcinoma. *Oncology letters*, 24(4), 351.

- [52] Hu D, Meng N, Lou X, et al., 2021. Prognostic Values of E2F1/2 Transcriptional Expressions in Chromophobe Renal Cell Carcinoma Patients: Evidence from Bioinformatics Analysis. *International journal of general medicine*, 14, 3593–3609.
- [53] Teissier S, Pang C, Thierry F, 2010, The E2F5 Repressor Is an Activator of E6/E7 Transcription and Of The S-Phase Entry in HPV18-Associated Cells. *Oncogene*, 29(36): 5061–5070.
- [54] Lin C, Hu Z, Yuan G, et al., 2018, MicroRNA-1179 Inhibits the Proliferation, Migration and Invasion of Human Pancreatic Cancer Cells by Targeting E2F5. *Chemico-Biological Interactions*, 291: 65–71.
- [55] Liu Y, Liu D, Wan W, 2019, MYCN-Induced E2F5 Promotes Neuroblastoma Cell Proliferation Through Regulating Cell Cycle Progression. *Biochemical And Biophysical Research Communications*, 511: 35–40.
- [56] Ali A, Ali A, Khan S, et al., 2021, Inhibition of HDACs Suppresses Cell Proliferation and Cell Migration of Gastric Cancer by Regulating E2F5 Targeting BCL2. *Life (Basel)*, 11(12): 1425.

Publisher's note

Bio-Byword Scientific Publishing remains neutral with regard to jurisdictional claims in published maps and institutional affiliations.

Multivariable Mendelian Randomization Analysis Reveals Potential Causal Effects between Immune Cells and Prostate Cancer Risk

Bin Hu¹, Haiqin Luo¹, Zhangcheng Liu^{2*}

¹Department of Urology, Kweichow Moutai Hospital, Zunyi 564500, Guizhou, China

²Department of Urology, The Second People's Hospital of Neijiang, Neijiang 641000, Sichuan, China

*Corresponding author: Zhangcheng Liu, DocLZC@163.com

Copyright: © 2025 Author(s). This is an open-access article distributed under the terms of the Creative Commons Attribution License (CC BY 4.0), permitting distribution and reproduction in any medium, provided the original work is cited.

Abstract: *Background:* Previous studies indicated that immune cells and Metabolites might play an important role in the occurrence and development of Prostate Cancer (PCa). Our study aimed to illustrate the causal effects between immune cells and metabolites and PCa risk, and the mediating role of metabolites between immune cells and PCa. *Methods:* This study utilized immune cells as Exposures, metabolites as Mediators, and PCa as Outcomes. Initially, immune cell and metabolite data were processed. Subsequently, a four-stage approach involved six Mendelian randomization analyses: Stage one focused on batch immune cell to PCa MR (MR 1); Stage two involved immune cell to PCa Reverse MR (MR 2); Stage three performed batch metabolite to PCa MR (MR 3); Stage four included three MR analyses: prostate carcinogenesis related immune cells to PCa-related metabolites MR yielding beta 1 (MR 4), PCa-related metabolites to PCa MR yielding beta 2 (MR 5), and prostate carcinogenesis related immune cells to PCa MR yielding beta All (MR 6). Finally, mediation and direct effects were computed. *Results:* Our research identified twenty-five immune cells and nine metabolites associated with the incidence of PCa. Among the most intriguing associations, genetically predicted “CD25 on IgD⁺ CD38⁻ Unswitched Memory (unsw mem) cells” are linked to an increased risk of PCa, Notably, 14.6% (1.68%, 27.5%) of this risk is mediated through the metabolite “3-hydroxypyridine sulfate levels” with a mediated effect of 0.00235 (0.00027, 0.00442) and a p-value of 0.026751157. This indicates that an increase in “CD25 on IgD⁺ CD38⁻ unsw mem cells” can promote the development of PCa by reducing the levels of “3-hydroxypyridine sulfate”. *Conclusions:* Our findings suggest that 3-hydroxypyridine sulfate mediates the association between CD25 on IgD⁺ CD38⁻ unsw mem and increased PCa risk. This study unexpectedly found that elevated 3-hydroxypyridine sulfate levels may explain how coffee consumption could protect against PCa.

Keywords: Mendelian randomization; Prostate cancer (PCa); Immune Cells; Metabolites; 3-hydroxypyridine sulfate; CD25 on IgD⁺ CD38⁻ unswitched memory (unsw mem) cells

Online publication: Oct 21, 2025

1. Introduction

PCa is a significant global health concern, with approximately 1.3 million new cases diagnosed each year. Currently, there are around 10 million men living with a PCa diagnosis, with about 700,000 of them having metastatic disease. Metastatic PCa is responsible for over 400,000 deaths yearly, and this number is projected to more than double by 2040 ^[1]. Therefore, it is imperative to research the molecular mechanisms underlying its development, identify the root causes of the disease, and ultimately work towards preventing its occurrence.

Recent research published in *Nature* highlights that immune cells can identify cancer cell antigens and present them to T cells and B cells for elimination ^[2]. Despite PCa typically being considered an immunologically “cold” tumor, it is indeed infiltrated by various types of immune cells ^[3]. Studies on the immune-related microenvironment indicate that both innate and adaptive immune cells play roles in the development and progression of PCa ^[4].

Additionally, previous study identified 103 genes associated with immune cell abundance in the tumor microenvironment, illustrating how genetic variations influence the expression of immune genes ^[5]. Immune cells, especially B cells, undergo various genetic stresses during their maturation and activation processes ^[6]. Double-strand DNA breaks and mutations are crucial for normal immune function; however, improper management of these DNA damages can lead to serious consequences such as immune deficiencies or cancer ^[7]. These findings collectively underscore how genetic factors may impact the expression and infiltration of immune cells, thereby potentially influencing the onset and progression of PCa.

Furthermore, relevant investigations have demonstrated a possible relationship between plasma metabolite concentrations and PCa risk ^[8]. Studies discovered that 49 metabolites were related with PCa survival ^[9]. As lipid metabolism contributes to the progression of PCa and citrulline metabolites may signal subclinical PCa ^[10–12]. While lignans and in vivo metabolites, particularly enterolactone (ENL), may be employed as chemo-preventive treatments for PCa ^[13]. Vitamin D and its metabolites can help cure and prevent PCa ^[14]. L-methionine (l-Met) and its metabolites play an important role in the development of PCa ^[15].

Metabolites are highly hereditary, where relevant studies have revealed that the expression of metabolites is affected by genetics, epigenetics, and the environmental factors ^[16–19]. At the same time, Metabolite concentrations are influenced by both genetic and environmental factors ^[20]. However, there is still absence of research investigating the potential causal relationship between immunity and metabolism in the pathogenesis of PCa.

Mendelian randomization (MR) serves as a causal inference technique that leverages genetic variants as a surrogate for exposure, resembling a natural randomized controlled trial and mitigating confounding bias and reverse causality often present in observational studies. Multivariable Mendelian randomization (MVMR) is an extended method that enables the investigation of independent effects of correlated exposures on an outcome by include genetic variations of each exposure in the same model. Additionally, since traditional, non-instrumental variable methods for mediation analyses would experience bias due to confounding between an exposure, mediator, and outcome as well as measurement error, a two-step MVMR study can be used to investigate the pathways through which an exposure affects an outcome and improve causal inference in mediating effects ^[21].

This study examined the independent causal relationships between immune cells and metabolites in the development of PCa, utilizing immune cells as exposure factors, metabolites as mediating factors, and PCa as outcome factors. The focus was on the mediating effect of metabolites on alterations in immune cell numbers during the pathogenesis of PCa, providing a foundation for further research on the disease.

2. Methods

2.1. Study design

This study utilized immune cells as Exposures, metabolites as Mediators, and PCa as Outcomes. Initially, immune cell and metabolite data were processed by correlational analysis of genetic factors and exposures, removal of linkage disequilibrium Single Nucleotide Polymorphisms (SNPs), and exclusion of weak instrumental variables. Subsequently, a four-stage approach involved six Mendelian randomization analyses: First, MR Analysis of batch immune cells to PCa (MR 1). Second, the Reverse MR Analysis: PCa was sent to immune cells for MR Analysis (MR 2). Third, the MR Analysis of batch metabolites to PCa (MR 3). Then, the mediating effect analysis included three MR Analyses including the MR Analysis of prostate carcinogenesis related immune cells (MR 4), the MR Analysis of PCa-related metabolites to PCa (MR 5) and the MR Analysis of prostate carcinogenesis related immune cells of PCa to NAFLD (MR 6). Finally, mediation and direct effects were computed. The research ideas are detailed in **Figure 1**.

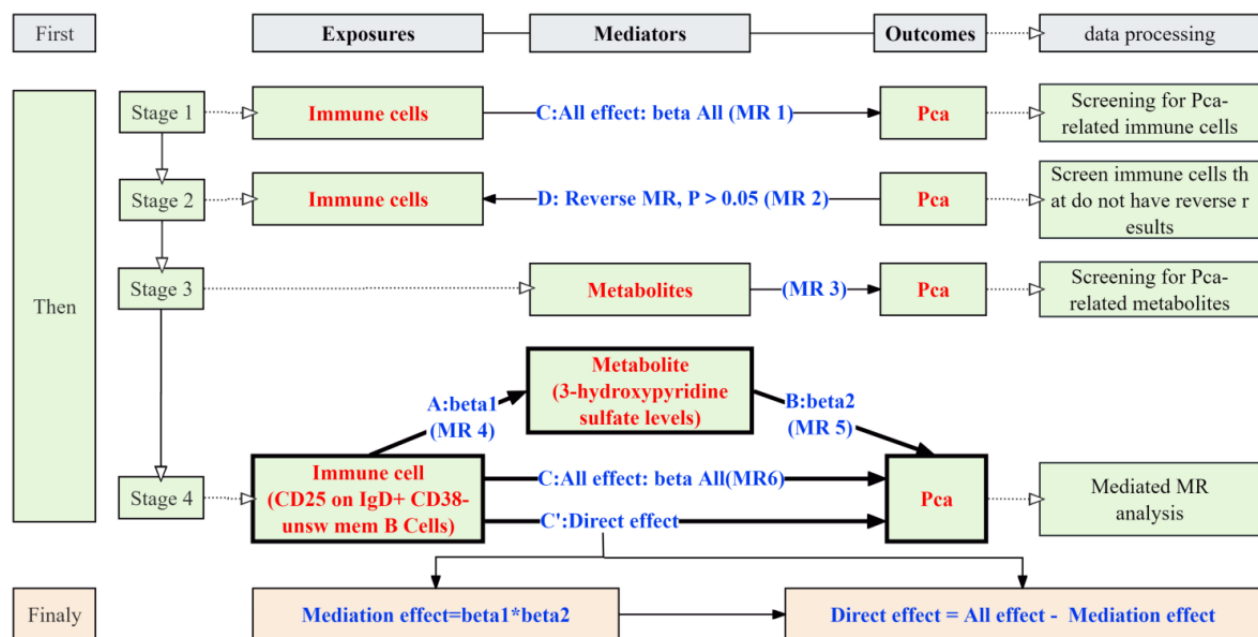


Figure 1. Overview of the study design.

2.2. Data sources of exposures, mediators, and outcomes

The PCa data of the European population published in 2021 from the Genome-Wide Association Study (GWAS) summary data (<https://gwas.mrcieu.ac.uk/datasets/ebi-a-GCST90018905/>) was obtained, with a total of 211227, and the sample size, 24119306 Number of SNPs^[22]. The immune cell data of the European population from the literature was downloaded, including a total of 731 immune cells, numbers from GCST0001391 (<https://www.ebi.ac.uk/gwas/studies/GCST0001391>) to the GCST0002121 (<https://www.ebi.ac.uk/gwas/studies/GCST0002121>)^[21]. The metabolite data of the European population from the literature was downloaded, including a total of 1399 metabolites and 34843 SNPs this data which was accessible and available at (http://ftp.ebi.ac.uk/pub/databases/gwas/summary_statistics/)^[23]. The above three sets of data were selected from populations of European ancestry to reduce potential bias from population stratification.

This study utilized the R 4.3.2 TwoSampleMR package to filter data with a p-value $< 1 \times 10^{-5}$, extracting

SNPs strongly correlated with “immune cells or metabolites”. Parameters were set to $kb = 10000$ and $r^2 = 0.001$ to filter out SNPs in linkage disequilibrium. Using the ‘ieugwasr’ R package, and removed weak instrumental variables (defined as those poorly correlated with the phenotype or explaining minimal phenotype variance, with $F < 10$).

2.3. MR of batch immune cells or metabolites to PCa (Step one, three)

To identify immune cells and metabolites associated with PCa, Mendelian randomization analyses were conducted using the TwoSampleMR, version 0.42, R package. Five methods (MR Egger, Weighted median, Inverse variance weighted (IVW), Simple mode, Weighted mode) were employed for batch MR analysis of immune cell datas or metabolites to PCa, with IVW as the primary method [24]. Results were filtered using p -value < 0.05 , and immune cells and metabolites showing consistent directional odds ratios ($OR > 1$ or $OR < 1$) across all five MR methods were finally extracted.

2.4. Reverse MR of Immune cells to PCa (Step two)

To screen for immune cells associated with the pathogenesis of PCa, MR Analysis (MR 2) was performed in this study, where the reverse MR Analysis of immune cells to NAFLD, using PCa as the exposure factor and immune cells as the outcome variable. Pleiotropy results were filtered with $p > 0.05$ to obtain negative results, and immune cells with $p < 0.05$ were excluded.

2.5. Mediation MR (Step four)

In Steps one to three, Mendelian Randomization (MR1,2,3) was used to identify prostate carcinogenesis related immune cells and PCa related metabolites. In Step four, three MR analyses was concluded including the MR (MR4) of prostate carcinogenesis related immune cells on PCa related metabolites to identify metabolites mediating the effect of immune cells on PCa development, obtain effect size β_{12} . Next is MR (MR5) of PCa related metabolites on PCa to obtain effect size β_2 . Then is MR (MR6) of prostate carcinogenesis related immune cells on PCa to obtain total effect size β_{all} . For these analyses, this study has employed the TwoSample MR package and applied the MR-PRESSO method for pleiotropy testing to identify and remove biased SNPs (significance level < 0.05) [25]. Then performed heterogeneity testing, created scatter plots, forest plots, and funnel plots and conducted a Leave one out analysis. Finally, calculate the mediating effect $\beta_{12} = \beta_1 \times \beta_2$, direct effect ($\beta_{dir} = \text{total effect } (\beta_{all}) - \text{mediating effect } (\beta_1 \times \beta_2)$).

3. Result

3.1. Screening of PCa-associated immune cells

In Step one, 731 immune cells were referred from the literature. After removing invalid instrumental variables, this study further filtered it down to 729 immune cells. Using five different Mendelian Randomization (MR1) analysis methods, and 34 immune cells was identified to have a causal relationship with PCa. Further screening revealed 26 immune cells with consistent OR directions and p -value < 0.05 across all five MR methods.

In Step two, reverse Mendelian Randomization analysis was used to identify 25 prostate carcinogenesis related immune cells (p -value > 0.05) for subsequent mediation Mendelian Randomization (MR2) analysis. These immune cells include IgD^+CD38^- %lymphocyte, $CD62L^-$ monocyte %monocyte, $CD39^+$ resting Treg AC, Secreting Treg % CD4 Treg, Activated & resting Treg % CD4 Treg, Monocytic Myeloid-Derived Suppressor

Cell (Mo MDSC AC), CD14⁻ CD16⁺ monocyte %monocyte, Leukocyte AC, CD8br NKT %T cell, CD24 on IgD⁺ CD24⁺, CD24 on IgD⁻ CD38⁻, CD24 on unsw mem, CD25 on IgD⁺ CD38⁻ unsw mem, IgD on IgD⁺ CD24⁻, CD3 on CD39⁺ resting Treg, HVEM on EM (effector memory) CD8br, HVEM on CD8br, CD4 on monocyte, FSC-A (forward scatter area) on plasmacytoid dendritic cell (DC), FSC-A on NK, Side Scatter Area (SSC-A) on granulocyte, CD11c on myeloid DC, CD11c on CD62L⁺ myeloid DC, HLA DR on DC, and HLA DR on CD33dim HLA DR⁺ CD11b⁻.

3.2. Screening of PCa-associated metabolites

In Step three, 1400 metabolites were initially obtained from the literature. After removing instrumental variables, 1400 metabolites were screened. Further analysis using five Mendelian randomization (MR3) methods identified 1399 metabolites with potential causal relationships to PCa. Among these, 9 metabolites consistently showed odds ratios (OR) and p-value ≤ 0.05 across all five MR methods. These metabolites include Cysteinyl glycine disulfide, 3-hydroxypyridine sulfate, Sulfate of piperine metabolite C₁₆H₁₉NO₃, Sarcosine, oxidized Cys-gly, Arachidonate (20:4, n-6), X-19438, Phosphate to citrate ratio, and the ratio of Androsterone glucuronide to Etiocholanolone glucuronide.

3.3. The mediation Mendelian randomization analysis

In Steps one to three, prostate carcinogenesis-related immune cells and PCa related metabolites were screened for potential use in intermediate Mendelian randomization analysis. Subsequently, in step four, three Mendelian randomization analyses were conducted.

3.3.1. Result of prostate carcinogenesis related immune cells to PCa-related metabolites MR (MR 4)

A causal relationship between prostate carcinogenesis-related immune cells (CD25 on IgD⁺ CD38⁻ unsw mem) and the PCa-related metabolites (3-hydroxypyridine sulfate levels, CST90199990) was discovered. All five MR methods showed a beta (β) value of < 0 , with the IVW method presenting a p-value of < 0.05 and an OR value of < 1 . Combining the scatter plot and forest plot, the analysis indicates that CD25 on IgD⁺ CD38⁻ unsw mem is a protective factor for 3-hydroxypyridine sulfate levels. As the number of CD25 on IgD⁺ CD38⁻ unsw mem increases, the levels of 3-hydroxypyridine sulfate decrease; conversely, as the number of CD25 on IgD⁺ CD38⁻ unsw mem decreases, the levels of 3-hydroxypyridine sulfate increase. The leave-one-out analysis suggests that the MR analysis results are reliable and stable. The funnel plot analysis shows no heterogeneity of SNPs. For further details, see **Figure 2**.

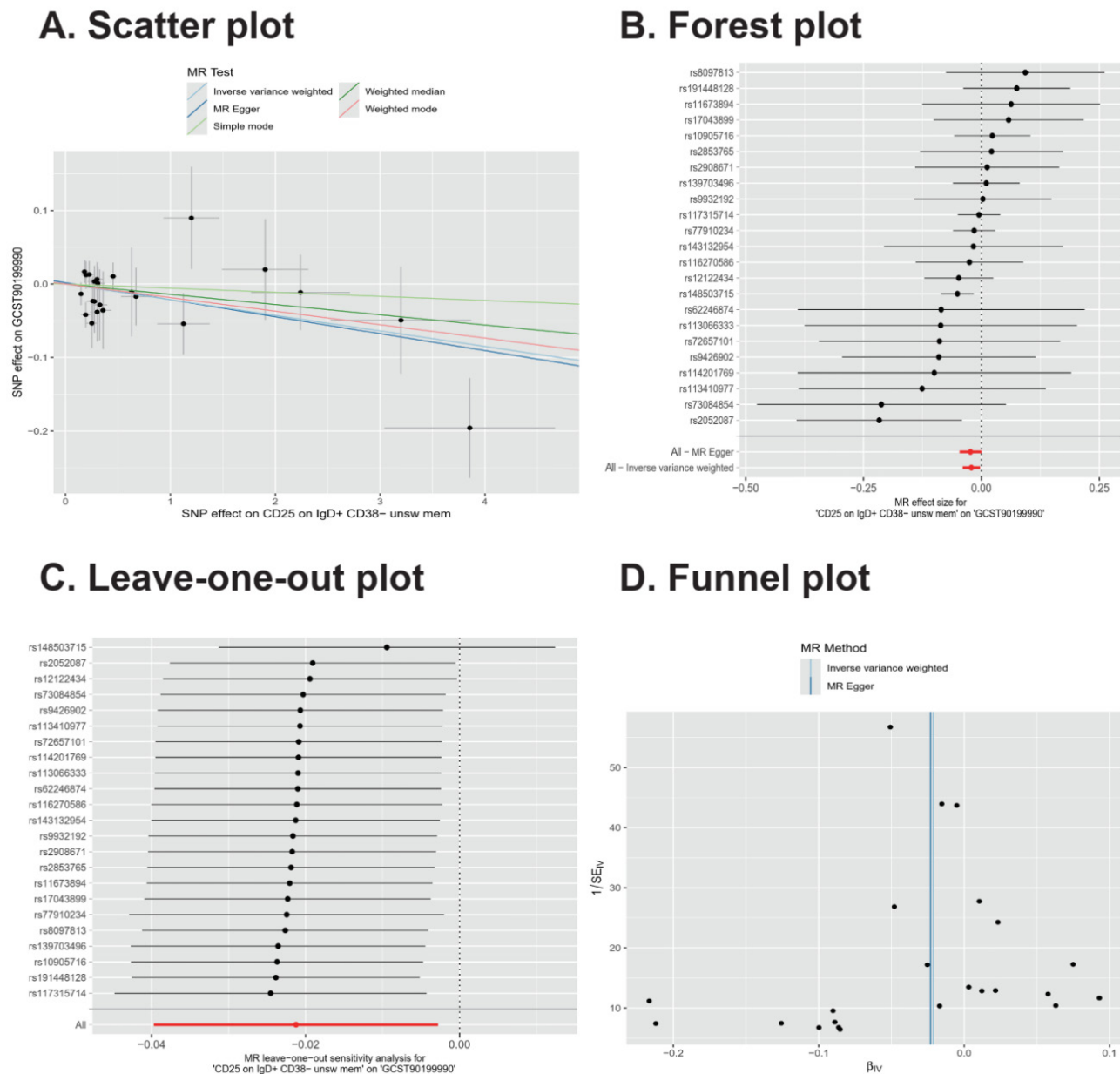
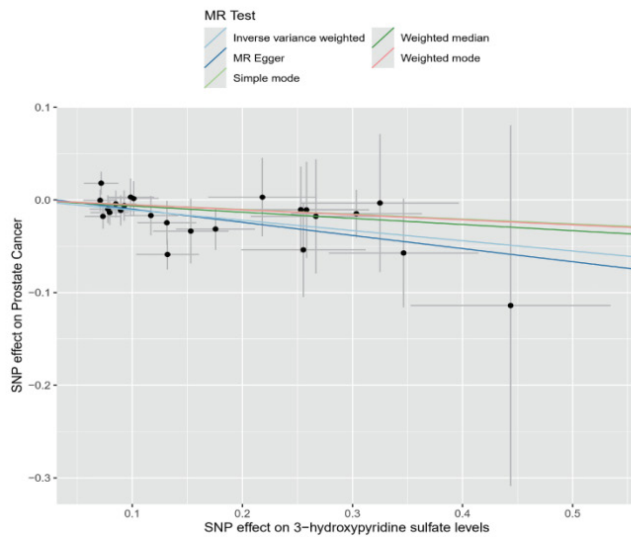


Figure 2. CD25 on IgD+ CD38- unsw mem on 3-hydroxypyridine sulfate levels of MR analysis result. A. Scatter plot; B. Forest plot of SNP; C. Leave one-out-plot plot; D. Funnel plot.

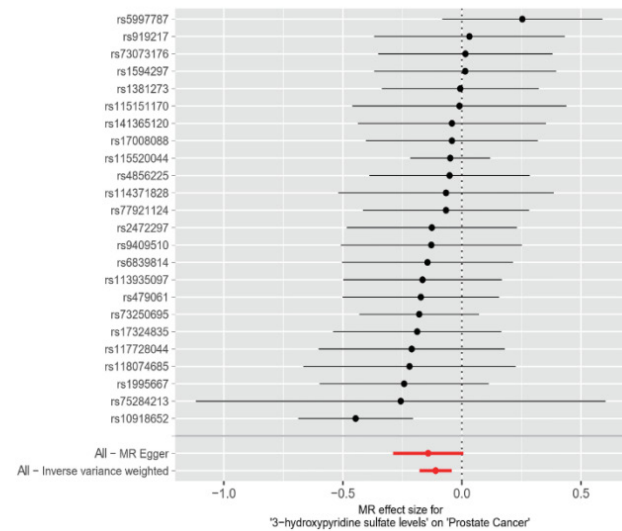
3.3.2. Result of PCa-related metabolites to PCa MR (MR 5)

Through analysis, it was discovered that there is a causal relationship between PCa-related metabolites (3-hydroxypyridine sulfate levels) and PCa. The b (beta 1) values of all five methods were < 0 , the p value of the IVW method was < 0.05 , and the OR < 1 . Combined with the scatter plot and forest plot, the analysis indicates that “3-hydroxypyridine sulfate levels” are a protective factor for PCa. As the levels of “3-hydroxypyridine sulfate levels” increase, the risk of PCa decreases; conversely, as the levels decrease, the risk of PCa increases. The leave-one-out analysis demonstrated the reliability and stability of the MR analysis results. The funnel plot analysis indicated that the SNPs do not exhibit heterogeneity. For further details, refer to **Figure 3**.

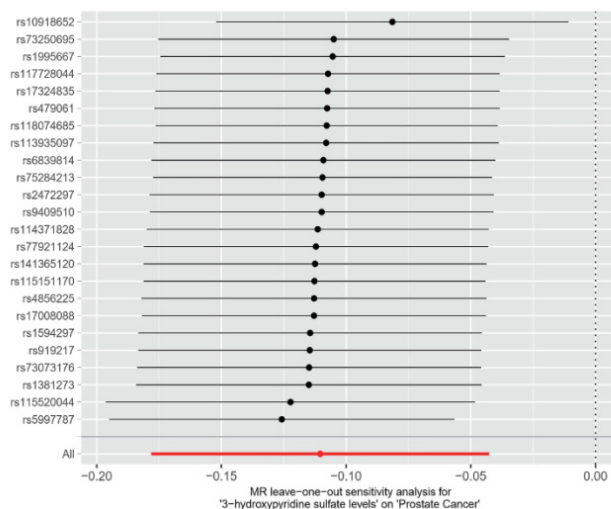
A. Scatter plot



B. Forest plot



C. Leave-one-out plot



D. Funnel plot

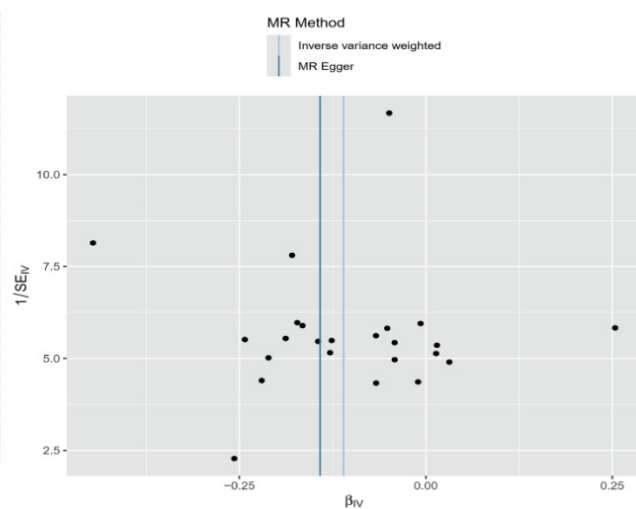


Figure 3. 3-hydroxypyridine sulfate levels on PCa of MR analysis result. A. Scatter plot; B. Forest plot of SNP; C. Leave one-out-plot plot; D. Funnel plot.

3.3.3. Result of prostate carcinogenesis related immune cells to PCa MR (MR 6)

A causal relationship between prostate carcinogenesis and immune cells expressing “CD25 on IgD⁺ CD38⁻ unsw mem” was discovered. The b (beta 1) values of all five methods were > 0 , with the IVW method showing a p-value < 0.05 and an OR > 1 . Combined scatter plot and forest plot analyses indicate that “CD25 on IgD⁺ CD38⁻ unsw mem” is a risk factor for PCa. As the quantity of “CD25 on IgD⁺ CD38⁻ unsw mem” increases, the risk of PCa also increases; conversely, a decrease in “CD25 on IgD⁺ CD38⁻ unsw mem” quantity lowers the risk. Leave-one-out analysis demonstrates the reliability and stability of MR analysis results. Funnel plot analysis shows no heterogeneity in SNP. See **Figure 4** for details.

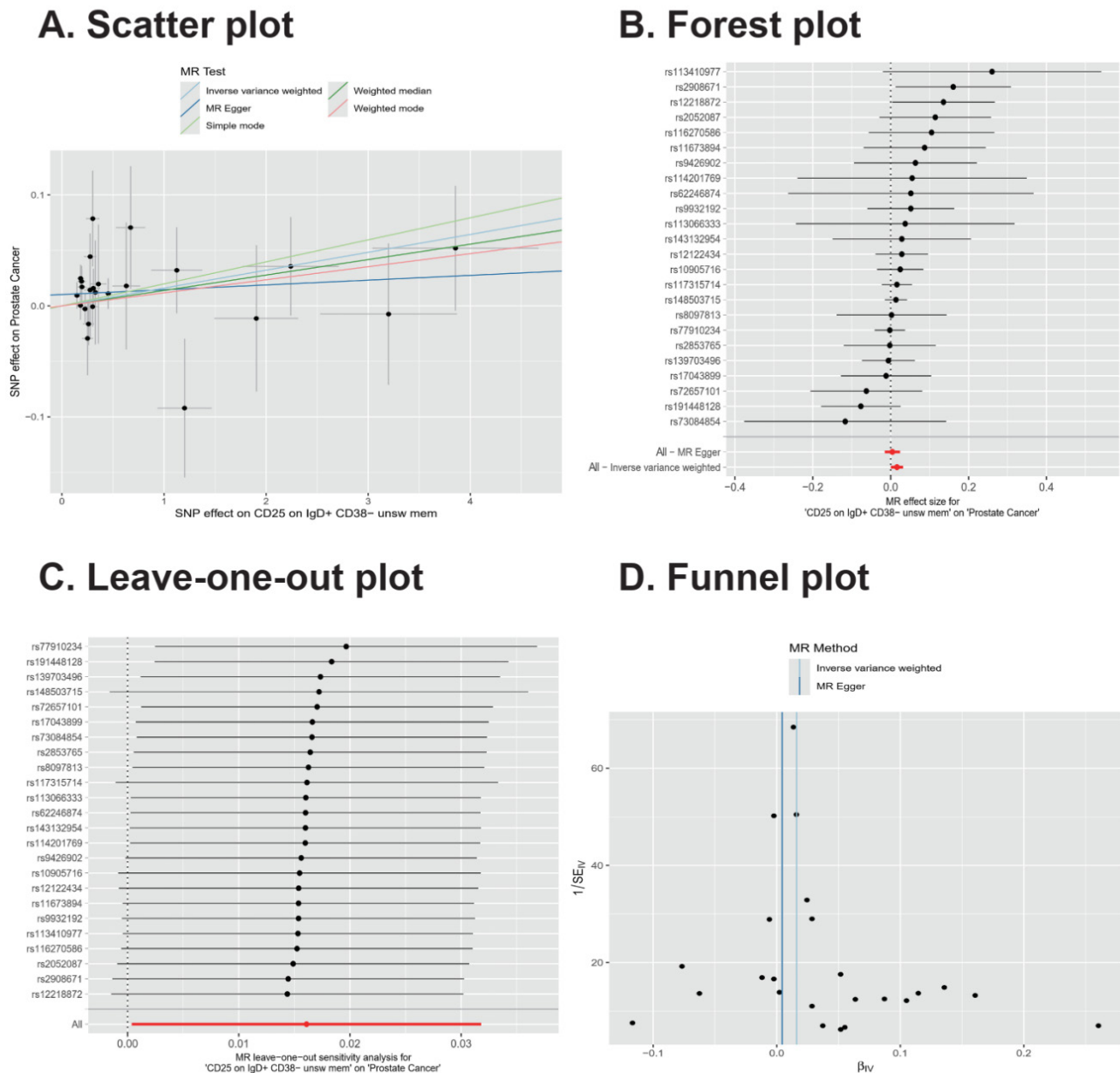


Figure 4. CD25 on IgD⁺ CD38⁻ unsw mem on PCa of MR analysis result. A. Scatter plot; B. Forest plot of SNP; C. Leave one-out-plot; D. Funnel plot.

3.3.4. Mediation effect, mediation ratio, and direct effect

Based on the formula: Mediation effect (β_{12}) = $\beta_{11} \times \beta_{21}$, Direct effect (β_{dir}) = Total effect (β_{all}) – Mediation effect (β_{12}), the mediated effect is 0.00235 (0.00027, 0.00442), the mediated proportion is 14.6% (1.68%, 27.5%), and the p-value is 0.026751157 (**Table 1**). The direct effect is 0.0137478280. In each of the three Mendelian randomization analyses conducted, the IVW method demonstrated a p-value < 0.05. The initial two analyses revealed an odds ratio (OR) < 1, while the third analysis exhibited an OR > 1. This indicates that an increase in the number of “CD25 on IgD⁺ CD38⁻ unswitched memory B cells” can promote the occurrence of PCa by reducing “3-hydroxypyridine sulfate levels”, with a mediation effect of 14.6%, which is statistically significant.

See **Figure 5** for details.

Table 1. Multivariable Mendelian randomization and mediation analyses result OF CD25 on IgD⁺ CD38⁺ unsw mem, 3-hydroxypyridine sulfate levels and PCa

| Immune cell | Metabolite | Outcome | Mediated effect | Mediated proportion | p-value |
|---|----------------------------------|---------|----------------------------|----------------------|-------------|
| CD25 on IgD ⁺ CD38 ⁺ unsw mem | 3-hydroxypyridine sulfate levels | PCa | 0.00235 (0.00027, 0.00442) | 14.6% (1.68%, 27.5%) | 0.026751157 |

| exposure | outcome | nsnp | method | pval | OR(95% CI) |
|---|-----------------|------|---------------------------|--------------|------------------------|
| CD25 on IgD ⁺ CD38 ⁺ unsw mem | GCST90199990 | 23 | MR Egger | 0.065 | 0.977 (0.955 to 1.000) |
| | | 23 | Weighted median | 0.361 | 0.986 (0.957 to 1.016) |
| | | 23 | Inverse variance weighted | 0.024 | 0.979 (0.961 to 0.997) |
| | | 23 | Simple mode | 0.809 | 0.994 (0.951 to 1.040) |
| | | 23 | Weighted mode | 0.225 | 0.982 (0.954 to 1.011) |
| 3-hydroxypyridine sulfate levels | Prostate Cancer | 24 | MR Egger | 0.073 | 0.868 (0.749 to 1.006) |
| | | 24 | Weighted median | 0.202 | 0.936 (0.845 to 1.036) |
| | | 24 | Inverse variance weighted | 0.001 | 0.896 (0.837 to 0.958) |
| | | 24 | Simple mode | 0.560 | 0.950 (0.800 to 1.127) |
| | | 24 | Weighted mode | 0.488 | 0.948 (0.816 to 1.101) |
| CD25 on IgD ⁺ CD38 ⁺ unsw mem | Prostate Cancer | 24 | MR Egger | 0.672 | 1.004 (0.985 to 1.024) |
| | | 24 | Weighted median | 0.207 | 1.014 (0.992 to 1.036) |
| | | 24 | Inverse variance weighted | 0.045 | 1.016 (1.000 to 1.032) |
| | | 24 | Simple mode | 0.242 | 1.020 (0.988 to 1.054) |
| | | 24 | Weighted mode | 0.252 | 1.012 (0.992 to 1.032) |

Figure 5. Forest plot of multivariable Mendelian randomization and mediation analyses result for CD25 on IgD⁺ CD38⁺ unsw mem, 3-hydroxypyridine sulfate levels and PCa.

4. Discussion

Previous studies indicated that immune cells and metabolites might play an important role in the occurrence and development of PCa^[12,26–29]. Our study aimed to illustrate the causal effects between immune cells and metabolites and PCa risk, and the mediating role of metabolites between immune cells and PCa. Our results suggested that 25 immune cells and 9 metabolites were associated with PCa. The most intriguing correlation is with the genetically predicted “CD25 on IgD⁺ CD38⁺ Unswitched Memory B cells” was associated with an increased risk of PCa, and 14.6% (1.68%, 27.5%) of this effect was mediated through Metabolite “3-hydroxypyridine sulfate levels”.

This research have first identified that the expression level of “CD25 on IgD⁺ CD38⁺ Unswitched Memory B cells” correlates with an elevated risk of PCa incidence. Relevant studies have manifested that compared to the normal prostate tissue, higher B cell infiltration was found in the PCa regions, suggesting that B cells can facilitate the development of PCa and serve as a therapeutic target^[30]. According to the expression levels of IgM, IgD, CD10, CD19, CD24, CD27 and CD38, B cells could be divided into eight continuous differentiated subsets, namely Immature B cells, T1 Transitional B cells, T2 Transitional B cells, T3 Transitional B cells, Naive B cells, unswitched-memory B cells (unsw-mem B), switched-memory B cells (unsw-mem B), Plasmablast cells^[31,32]. Many studies refer to cells with either the phenotype CD27⁺IgM⁺IgD⁺ or CD27⁺IgM⁺IgD[−] as unswitched memory B cells. Among them, IgD serves as a marker for regulatory B cells involved in negative regulation of immune and inflammatory responses; CD38 is a multifunctional receptor and enzyme present on the surface of B lymphocytes^[33,34]. It influences B cell functions by cross-linking with relevant cytokines, inducing B lymphocyte proliferation and apoptosis, thereby

affecting immune regulation in the body and promoting tumorigenesis; and CD25 is activated B cell markers, one study shown that CD25 expresses at high level in B-ALL patients with BCR/ABL⁽⁺⁾, which may serve as a predictive marker for the presence of BCR/ABL fusion gene, and relates with relapse, CD25⁽⁺⁾ may serve as an adjuvant indicator for poor prognosis^[35,36]. Therefore, based on the above studies, it is reasonable to hypothesize that elevated levels of CD25 expression on IgD⁺ CD38⁻ Unswitched Memory B cells may indicate a poor prognosis for the disease, which consistent with our research.

3-Hydroxypyridine sulfate serves as a serum marker for coffee consumption, has been reported to be associated with multiple diseases. One study found that the organic compound 3-hydroxypyridine sulfate was significantly associated with an increased risk of Diabetic retinopathy (DR), and some studies have shown that 3-hydroxypyridyl sulfate are inversely associated with the risk of asthma and primary gastric cancer^[37–40]. While there are currently no studies investigating the correlation between 3-hydroxypyridine sulfate and prostate cancer, numerous literature reports exist examining the relationship between coffee intake and prostate cancer. Some studies suggest an increased intake of coffee may be linked to a reduced risk of PCa, however, some studies indicate no clear evidence of an association with PCa incidence. Nevertheless, they collectively suggest that coffee consumption is associated with a reduced risk of fatal PCa, and possibly due to non-caffeine components of coffee^[41–44]. So, what are the main components of coffee consumption that play a protective role against prostate cancer? Our research may answer this question. Relevant studies have shown that 3-hydroxypyridine sulfate may affect the proliferation and apoptosis process of prostate cells by affecting the availability and activity of androgens^[45]. Future investigations, including prospective cohort studies and in vitro/in vivo experiments, are necessary to explore the association between levels of 3-hydroxypyridine sulfate in coffee metabolites in the blood and PCa. Such efforts aim to contribute to our understanding and prevention strategies against PCa.

For the first time, 3-hydroxypyridine sulfate was identified to mediate the effect of “CD25 on IgD⁺ CD38⁻ Unswitched Memory B cells” on the onset of prostate cancer. The mechanism may be that 3-hydroxypyridine sulfate affects CD25 expression level in the context of B cell activation and memory formation^[46].

A multivariate Mendelian randomization (MVMR) approach was used to analyze the results, which is similar to a natural randomized controlled trial, which avoids the confounding bias and reverse causality of some observational studies, and also incorporates the genetic variants of each exposure into the same model to investigate the independent effects of related exposures on the results. The results are consistent with those of previous studies. To date, this study are the first to investigate the causal relationship between immune cells and metabolites and the risk of PCa, and our study is also the first to demonstrating that the number of CD25 on IgD⁺ CD38⁻ Unswitched Memory B cells increase, which may increase the risk of PCa by reducing 3-hydroxypyridine sulfate levels.

However, the study has three limitations. Firstly, our analysis is based solely on European populations, which may limit the generalizability of our findings to other regions^[21–23]. In future studies, including populations from other regions for analysis should be considered. Secondly, our prostate cancer data only discussed overall prostate cancer cases and did not perform clinical staging of prostate cancer. Thirdly, our study shows that 3-hydroxypyridine sulfate levels mediated genetic prediction in PCa rate of 14.6%, still needs more research to quantify other medium.

5. Conclusion

In summary, this study revealed the causal relationship between immune cells and metabolites and PCa through

mediated Mendelian randomization analysis, and findings indicate that 3-hydroxypyridine sulfate levels mediate the observed association between CD25 on IgD⁺ CD38⁺ unsw mem and heightened risk of PCa. This study speculate that increased levels of the metabolite 3-hydroxypyridine sulfate may serve as a potential mechanism by which coffee consumption exerts a protective effect against the occurrence or progression of PCa. This hypothesis presented novel avenues for future research in this field.

Funding

A Study to Explore the Resistance Mechanism of Carbapenem Resistant *Escherichia coli* in Patients with Urinary Sepsis Based on Bacterial Droplets Single Cell RNA-Seq (Project No.: MTyk2024-34)

Disclosure statement

The authors declare no conflict of interest.

Reference

- [1] Sandhu S, Moore C, Chiong E, et al., 2021, Prostate Cancer. *Lancet*, 398(10305): 1075–1090.
- [2] Baranov P, Atkins J, 2022, Immune Cells Alter Genetic Decoding in Cancer. *Nature*, 603(7902): 582–583.
- [3] Classon J, Zamboni M, Engblom C, et al., 2022, Prostate Cancer Disease Recurrence After Radical Prostatectomy is Associated with HLA Type and Local Cytomegalovirus Immunity. *Molecular Oncology*, 16(19): 3452–3464.
- [4] Jin K, Qiu S, Chen B, et al., 2023, DOK3 Promotes Proliferation and Inhibits Apoptosis of Prostate Cancer via the NF-KappaB Signaling Pathway. *Chinese Medical Journal*, 136(4): 423–432.
- [5] Lim Y, Chen-Harris H, Mayba O, et al., 2018, Germline Genetic Polymorphisms Influence Tumor Gene Expression and Immune Cell Infiltration. *Proceedings of the National Academy of Sciences of the United States of America*, 115(50): E11701–E11710.
- [6] An L, Wang Y, Liu Y, et al., 2010, Rad9 is Required for B Cell Proliferation and Immunoglobulin Class Switch Recombination. *Journal Of Biological Chemistry*, 285(46): 35267–35273.
- [7] Xu Y, 2006, DNA Damage: A Trigger of Innate Immunity but a Requirement for Adaptive Immune Homeostasis. *Nature Reviews Immunology*, 6(4): 261–270.
- [8] Rohnisch H, Kyro C, Olsen A, et al., 2020, Identification of Metabolites Associated with Prostate Cancer Risk: A Nested Case-Control Study with Long Follow-Up in the Northern Sweden Health and Disease Study. *BMC Medicine*, 18(1): 187.
- [9] Huang J, Zhao B, Weinstein S, et al., 2022, Metabolomic Profile of Prostate Cancer-Specific Survival Among 1812 Finnish Men. *BMC Medicine*, 20(1): 362.
- [10] Xu H, Li S, Sun Y, et al., 2021, ELOVL5-Mediated Long Chain Fatty Acid Elongation Contributes to Enzalutamide Resistance of Prostate Cancer. *Cancers (Basel)*, 13(16): 3957.
- [11] Matsushita M, Fujita K, Motooka D, et al., 2021, The Gut Microbiota Associated with High-Gleason Prostate Cancer. *Cancer Science*, 112(8): 3125–3135.
- [12] Schmidt J, Fensom G, Rinaldi S, et al., 2017, Pre-Diagnostic Metabolite Concentrations and Prostate Cancer Risk in 1077 Cases and 1077 Matched Controls in the European Prospective Investigation into Cancer and Nutrition. *BMC Medicine*, 15(1): 122.

- [13] Saarinen N, Tuominen J, Pylkkanen L, et al., 2010, Assessment of Information to Substantiate a Health Claim on the Prevention of Prostate Cancer by Lignans. *Nutrients*, 2(2): 99–115.
- [14] Swami S, Krishnan A, Feldman D, 2011, Vitamin D Metabolism and Action in the Prostate: Implications for Health and Disease. *Molecular and Cellular Endocrinology*, 347(1–2): 61–69.
- [15] Lu W, Saha A, Yan W, et al., 2020, Enzyme-Mediated Depletion of Serum L-Met Abrogates Prostate Cancer Growth via Multiple Mechanisms without Evidence of Systemic Toxicity. *Proceedings of the National Academy of Sciences of the United States of America*, 117(23): 13000–13011.
- [16] Hagenbeek F, Pool R, Van Dongen J, et al., 2020, Heritability Estimates for 361 Blood Metabolites across 40 Genome-Wide Association Studies. *Nature Communications*, 11(1): 39.
- [17] Matsuda F, 2016, Technical Challenges in Mass Spectrometry-based Metabolomics. *Mass Spectrometry (Tokyo)*, 5(2): S52.
- [18] Wells A, Barrington W, Dearth S, et al., 2022, Independent and Interactive Effects of Genetic Background and Sex on Tissue Metabolomes of Adipose, Skeletal Muscle, and Liver in Mice. *Metabolites*, 12(4): 337.
- [19] Zhu D, Wu X, Zhou J, et al., 2020, NuRD Mediates Mitochondrial Stress-Induced Longevity via Chromatin Remodeling in Response to Acetyl-CoA Level. *Science Advances*, 6(31): b2529.
- [20] Verri H, Dordevic N, Hantikainen E, et al., 2022, Age, Sex, Body Mass Index, Diet and Menopause Related Metabolites in a Large Homogeneous Alpine Cohort. *Metabolites*, 12(3): 205.
- [21] Orru V, Steri M, Sidore C, et al., 2020, Complex Genetic Signatures in Immune Cells Underlie Autoimmunity and Inform Therapy. *Nature Genetics*, 52(10): 1036–1045.
- [22] Sakaue S, Kanai M, Tanigawa Y, et al., 2021, A Cross-Population Atlas of Genetic Associations For 220 Human Phenotypes. *Nature Genetics*, 53(10): 1415–1424.
- [23] Chen Y, Lu T, Pettersson-Kymmer U, et al., 2023, Genomic Atlas of the Plasma Metabolome Prioritizes Metabolites Implicated in Human Diseases. *Nature Genetics*, 55(1): 44–53.
- [24] Matias-Garcia P, Wilson R, Guo Q, et al., 2021, Plasma Proteomics of Renal Function: A Transethnic Meta-Analysis and Mendelian Randomization Study. *Journal of the American Society of Nephrology*, 32(7): 1747–1763.
- [25] Verbanck M, Chen C, Neale B, et al., 2018, Detection of Widespread Horizontal Pleiotropy in Causal Relationships Inferred from Mendelian Randomization Between Complex Traits and Diseases. *Nature Genetics*, 50(5): 693–698.
- [26] Hayashi T, Fujita K, Matsushita M, et al., 2019, Main Inflammatory Cells and Potentials of Anti-Inflammatory Agents in Prostate Cancer. *Cancers (Basel)*, 11(8): 1153.
- [27] Jiang S, Li Z, Dou R, et al., 2022, Construction and Validation of a Novel Cuproptosis-Related Long Noncoding RNA Signature for Predicting the Outcome of Prostate Cancer. *Frontiers In Genetics*, 13: 976850.
- [28] Kocic G, Hadzi-Djokic J, Veljkovic A, et al., 2022, Template-Independent Poly(A)-Tail Decay and RNASEL as Potential Cellular Biomarkers for Prostate Cancer Development. *Cancers (Basel)*, 14(9): 2239.
- [29] Buszewska-Forajta M, Monedeiro F, Golebiowski A, et al., 2022, Citric Acid as a Potential Prostate Cancer Biomarker Determined in Various Biological Samples. *Metabolites*, 12(3): 268.
- [30] Zhang Y, Fu Y, 2021, Comprehensive Analysis and Identification of an Immune-Related Gene Signature with Prognostic Value for Prostate Cancer. *International Journal of General Medicine*, 14: 2931–2942.
- [31] Khoury J, Solary E, Abba O, et al., 2022, The 5th Edition of the World Health Organization Classification of Haematolymphoid Tumours: Myeloid and Histiocytic/Dendritic Neoplasms. *Leukemia*, 36(7): 1703–1719.
- [32] Wu X, Liu Y, Jin S, et al., 2021, Single-Cell Sequencing of Immune Cells from Anticitrullinated Peptide Antibody Positive and Negative Rheumatoid Arthritis. *Nature Communications*, 12(1): 4977.

- [33] Montorsi L, Siu J, Spencer J, 2022, B Cells in Human Lymphoid Structures. *Clinical and Experimental Immunology*, 210(3): 240–252.
- [34] Li Y, Li Z, Hu F, 2021, Double-Negative (DN) B Cells: An Under-Recognized Effector Memory B Cell Subset in Autoimmunity. *Clinical and Experimental Immunology*, 205(2): 119–127.
- [35] Zeng F, Zhang J, Jin X, et al., 2022, Effect of CD38 on B-Cell Function and its Role in the Diagnosis and Treatment of B-Cell-Related Diseases. *Journal of Cellular Physiology*, 237(7): 2796–2807.
- [36] Yang C, Yang L, Zhang R, et al., 2014, Expression of CD25 in Acute B Cell Lymphoblastic Leukemia and its Clinical Significance. *Zhongguo Shi Yan Xue Ye Xue Za Zhi*, 22(3): 634–639.
- [37] Chau Y, Au P, Li G, et al., 2020, Serum Metabolome of Coffee Consumption and its Association with Bone Mineral Density: The Hong Kong Osteoporosis Study. *Journal of Clinical Endocrinology and Metabolism*, 105(3): 210.
- [38] Fernandes S, Hokkanen J, Vangipurapu J, et al., 2023, Metabolites as Risk Factors for Diabetic Retinopathy in Patients with Type 2 Diabetes: A 12-Year Follow-up Study. *Journal of Clinical Endocrinology and Metabolism*, 109(1): 100–106.
- [39] Huang M, Kelly R, Chu S, et al., 2021, Maternal Metabolome in Pregnancy and Childhood Asthma or Recurrent Wheeze in the Vitamin D Antenatal Asthma Reduction Trial. *Metabolites*, 11(2): 65.
- [40] Shu X, Cai H, Lan Q, et al., 2021, A Prospective Investigation of Circulating Metabolome Identifies Potential Biomarkers for Gastric Cancer Risk. *Cancer Epidemiology Biomarkers and Prevention*, 30(9): 1634–1642.
- [41] Wang A, Wang S, Zhu C, et al., 2016, Coffee and Cancer Risk: A Meta-Analysis of Prospective Observational Studies. *Scientific Reports*, 6: 33711.
- [42] Wilson K, Kasperzyk J, Rider J, et al., 2011, Coffee Consumption and Prostate Cancer Risk and Progression in the Health Professionals Follow-up Study. *Journal of the National Cancer Institute*, 103(11): 876–884.
- [43] Yen C, Huang Y, Chung M, et al., 2022, Sugar Content and Warning Criteria Evaluation for Popular Sugar-Sweetened Beverages in Taipei, Taiwan. *Nutrients*, 14(16): 3339.
- [44] Discacciati A, Orsini N, Wolk A, 2014, Coffee Consumption and Risk of Nonaggressive, Aggressive and Fatal Prostate Cancer: A Dose-Response Meta-Analysis. *Annals of Oncology*, 25(3): 584–591.
- [45] Shiota M, Endo S, Tsukahara S, et al., 2024, Importance of 3 β -Hydroxysteroid Dehydrogenases and their Clinical use in Prostate Cancer. *Endocrine-Related Cancer*, 31(7): e240023.
- [46] Dirks J, Andres O, Paul L, et al., 2023, IgD Shapes the Pre-Immune Naïve B Cell Compartment in Humans. *Frontiers in Immunology*, 14: 1096019.

Publisher's note

Bio-Byword Scientific Publishing remains neutral with regard to jurisdictional claims in published maps and institutional affiliations.

The Effect of Body Temperature Flush Solution on Patients Undergoing Holmium Laser Lithotripsy via Ureteroscopy

Ming Xiong

Department of Urology, BOE Hospital, Suzhou 215200, Jiangsu, China

Copyright: © 2025 Author(s). This is an open-access article distributed under the terms of the Creative Commons Attribution License (CC BY 4.0), permitting distribution and reproduction in any medium, provided the original work is cited.

Abstract: *Objective:* To investigate the effect of isothermal flushing solution on the body temperature of patients undergoing holmium laser lithotripsy under ureteroscopy. *Method:* Thirty patients who underwent ureteroscopic holmium laser lithotripsy in our hospital from August 2024 to August 2025 were selected as the study subjects. They were randomly divided into an observation group and a control group using a random number table method, with 15 patients in each group. Among them, the observation group patients received intraoperative infusion of isothermal flushing solution, while the control group patients received intraoperative infusion of flushing solution at room temperature. Compare and analyze the changes in vital signs before and after surgery, temperature levels at different time points during surgery, and incidence of adverse reactions during the perioperative period between two groups of patients. *Result:* The postoperative central body temperature, mean arterial pressure, and heart rate of the observation group were significantly better than those of the control group ($p < 0.05$); The body temperature of observation groups T1, T2, and T3 was better than that of the control group; The incidence of adverse reactions was significantly lower than that of the control group ($p < 0.05$). *Conclusion:* The application of isothermal flushing solution in ureteroscopic holmium laser lithotripsy can improve the safety of the surgery, maintain the patient's body temperature during the operation, effectively reduce the occurrence of adverse reactions, and promote patient recovery.

Keywords: Body temperature flushing solution; Holmium laser lithotripsy under ureteroscopy; Body temperature

Online publication: Oct 21, 2025

1. Introduction

Holmium laser lithotripsy under ureteroscopy has become one of the mainstream surgical methods for treating ureteral stones due to its advantages of minimal trauma and precise efficacy. Continuous infusion of flushing solution during surgery can not only ensure clear surgical field of view, but also reduce the difficulty of removing debris. However, under the influence of long-term and large infusion of flushing solution at room temperature, the fluctuation of the patient's core body temperature is significant, and hypothermia related

complications are prone to occur^[1].

At present, clinical research on how to maintain intraoperative body temperature stability by optimizing flushing fluid parameters is increasingly focused on, and the advantages of temperature flushing fluid are gradually becoming prominent. This article mainly explores the effect of isothermal flushing solution on the body temperature of patients undergoing holmium laser lithotripsy under ureteroscopy.

2. Data and methods

2.1. General Information

This experiment included a total of 30 patients who underwent holmium laser lithotripsy under ureteroscopy. Random number table method was used for group allocation, with a total of 15 patients participating in the control group, including 9 males/6 females; The average age is (45.21 ± 6.88) years old; For the average diameter of stones, this group had a diameter of (1.35 ± 0.41) cm; an additional 15 cases were included in the observation group, with 10 males/5 females; The average age is (46.13 ± 7.25) years old; The average diameter of the stones in this group was (1.38 ± 0.43) cm. There was no statistically significant difference in the above information between the two groups of patients ($p > 0.05$).

2.1.1. Inclusion criteria

- (1) Diagnosed with ureteral calculi through imaging examination, meeting the indications for holmium laser lithotripsy under ureteroscopy
- (2) ASA classification I-II
- (3) The body has no severe infection or other serious illness
- (4) The patients and their families are aware of the experimental procedures, objectives, etc. and express their willingness to cooperate

2.1.2. Exclusion criteria

- (1) Within the range of severe cardiovascular and cerebrovascular diseases
- (2) Abnormal coagulation function
- (3) Patients with preoperative fever or abnormal body temperature
- (4) People who are allergic to the components of the flushing solution

2.2. Method

In the intervention process for both groups of patients, tracheal intubation anesthesia was taken as the primary step, and the surgical operation was performed by the same group of medical staff. Ureteroscopy, holmium laser equipment, and surgical procedures were all the same.

The control group used room temperature flushing solution ($22\text{--}25\text{ }^{\circ}\text{C}$) for intraoperative perfusion, controlling the perfusion pressure. The pressure perfusion pump was used as the main tool to ensure that the index value was between $80\text{--}120\text{mmHg}$, and the perfusion speed was adjusted according to the clarity of the surgical field of view. The observation group used isothermal flushing solution for intraoperative perfusion, and the flushing solution was preheated to $37\text{ }^{\circ}\text{C}$ by a constant temperature heater, which was consistent with the core body temperature of the human body. The parameters such as perfusion pressure and speed were not different from those of the control group.

2.3. Observation indicators

2.3.1. Vital signs indicators

Select 10 minutes before and 10 minutes after surgery as monitoring and judgment time points, and compare the two groups based on accurate understanding of central body temperature, mean arterial pressure, and heart rate.

2.3.2. Intraoperative body temperature

Record the central body temperature of two groups of patients 10 minutes before surgery (T0), 30 minutes after surgery (T1), 60 minutes after surgery (T2), and at the end of surgery (T3).

2.3.3. Perioperative adverse reactions

Observe and record how many patients in each group experienced chills, nausea, vomiting, and worsening incision pain within 1 day after surgery, and use the total incidence rate as an important comparative indicator.

2.4. Statistical processing

SPSS 24.0 software was used to process the data. Count data was expressed as the number of cases (%) and subjected to a chi square test. Metric data was expressed as mean \pm standard deviation ($\bar{x} \pm s$) and subjected to a *t*-test. $p < 0.05$ was considered statistically significant.

3. Results

3.1. Comparison of vital signs indicators between two groups of patients

The vital signs of the observation group were more stable than those of the control group 10 minutes after surgery ($p < 0.05$), as shown in **Table 1**.

Table 1. Comparison of vital signs indicators between two groups of patients ($\bar{x} \pm s$)

| Group | Count down | Central body temperature (°C) | | Heart rate (Time/Min) | | Mean arterial pressure (mmHg) | |
|-------------------|------------|-------------------------------|-----------------------|-----------------------|-----------------------|-------------------------------|-----------------------|
| | | Pre-operative 10 min | Post-operative 10 min | Pre-operative 10 min | Post-operative 10 min | Pre-operative 10 min | Post-operative 10 min |
| Control group | 15 | 36.71 \pm 0.40 | 35.77 \pm 0.32 | 73.11 \pm 4.87 | 82.45 \pm 5.59 | 84.90 \pm 5.84 | 95.66 \pm 6.21 |
| Observation group | 15 | 36.80 \pm 0.36 | 36.69 \pm 0.27 | 72.59 \pm 5.34 | 75.17 \pm 4.98 | 85.23 \pm 6.12 | 87.04 \pm 5.74 |
| <i>t</i> -value | | 0.648 | 11.285 | 0.279 | 3.766 | 0.151 | 3.948 |
| <i>p</i> -value | | 0.522 | 0.000 | 0.783 | 0.001 | 0.881 | 0.000 |

3.2. Comparison of body temperature between two groups of patients at different time points during surgery

The body temperature of observation groups T1, T2, and T3 was better than that of the control group ($p < 0.05$), as shown in **Table 2**.

Table 2. Comparison of body temperature between two groups of patients at different time points during surgery ($^{\circ}\text{C}$, $\bar{x} \pm s$)

| Group | Countdown | T0 | T1 | T2 | T3 |
|-------------------|-----------|------------------|------------------|------------------|------------------|
| Control group | 15 | 36.72 ± 0.37 | 36.21 ± 0.30 | 35.89 ± 0.33 | 35.80 ± 0.32 |
| Observation group | 15 | 36.88 ± 0.32 | 36.71 ± 0.27 | 36.70 ± 0.22 | 36.59 ± 0.24 |
| <i>t</i> -value | | 1.267 | 4.798 | 7.910 | 7.649 |
| <i>p</i> -value | | 0.216 | 0.000 | 0.000 | 0.000 |

3.3. Comparison of perioperative adverse reaction rates between two groups of patients

In the comparison of the total incidence of adverse reactions, the observation group had a lower value ($p < 0.05$), as shown in Table 3.

Table 3. Comparison of perioperative adverse reaction rates between two groups of patients [n (%)]

| Group | Countdown | Shiver | Nausea and vomiting | Increased incision pain | Overall incidence rate |
|-------------------|-----------|--------|---------------------|-------------------------|------------------------|
| Control group | 15 | 3 | 2 | 1 | 6 (40.00) |
| Observation group | 15 | 0 | 1 | 0 | 1 (6.67) |
| χ^2 -value | | | | | 4.658 |
| <i>p</i> -value | | | | | 0.031 |

4. Discussions

Under ureteroscopy, holmium laser lithotripsy relies on continuous irrigation of flushing fluid to achieve clear surgical field and stone removal. However, the temperature difference between the flushing fluid and the body can easily cause heat exchange, leading to a decrease in core body temperature. The incidence of hypothermia is relatively high in this surgical procedure, mainly due to the flushing fluid taking away body heat, anesthesia inhibiting the thermoregulatory center, and closely related to surgical exposure. Low body temperature can activate the body's stress response, causing changes in heart rate and blood pressure in a stable state. It may also have an impact on immune function, which is not conducive to early postoperative recovery for patients [2]. Therefore, how to effectively maintain the intraoperative body temperature of patients undergoing ureteroscopic holmium laser lithotripsy is of great concern in clinical practice. The core of body temperature flushing solution refers to flushing products with a temperature that is consistent with the normal body temperature (about 37°C) to avoid stimulating sensitive parts of the body due to temperature differences. In ureteroscopic holmium laser lithotripsy, low-temperature flushing solution has a certain impact on the mucosal epithelial cells of patients, and the incidence of postoperative inflammatory reactions is relatively high. Waiting for the body temperature flushing solution to be consistent with the physiological environment of the mucosa can minimize irritation to the mucosa as much as possible.

The results of this study showed that the central body temperature of the observation group was (36.69 ± 0.27) $^{\circ}\text{C}$, the average arterial pressure was (87.04 ± 5.74) mmHg, and the heart rate was (75.17 ± 4.98) beats/min 10 minutes after surgery, all of which were better than the control group ($p < 0.05$). Moreover, the body

temperatures of T1, T2, and T3 were more stable than those of the control group ($p < 0.05$), indicating that equal temperature flushing solution can effectively reduce intraoperative heat loss, maintain stable core body temperature, and avoid significant impact on the circulatory system. Analysis of the reasons: The isothermal flushing solution is consistent with the core body temperature of the human body, which can avoid the “cold dilution” effect caused by continuous infusion of room temperature flushing solution, and is conducive to improving the imbalance between heat production and heat dissipation in the body thus achieving the goal of maintaining a steady body temperature^[3].

Compared with the 40.00% incidence of adverse reactions in the control group, 6.67% in the observation group was in a more ideal state ($p < 0.05$), further confirming the clinical advantages of isothermal flushing solution. The reason is that when the patient’s body temperature is in a stable state, the level of stress in the body gradually decreases, which increases the incidence of stress reactions such as chills, nausea, and vomiting. At the same time, avoiding the impact of low body temperature on local blood circulation at the incision site is of certain value for the patient’s early postoperative recovery.

5. Conclusion

In summary, among patients undergoing ureteroscopic holmium laser lithotripsy, the use of isothermal flushing solution has significant advantages and is one of the measures to maintain stable vital signs, avoid significant temperature drops at different time points during surgery, and reduce the possibility of symptoms such as chills, nausea, and vomiting. It is worth promoting and applying.

Disclosure statement

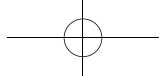
The author declares no conflict of interest.

References

- [1] Hu X, 2017, A Brief Discussion on the Effect of Isothermal Rinsing Liquid on Body Temperature and Blood Loss in Patients Undergoing Percutaneous Nephrolithotomy. *Contemporary Chinese Medicine*, 24(25): 63–65.
- [2] Peng L, 2016, Study on the Effect of Temperature Flushing Solution on the Body Temperature of Patients Undergoing Holmium Laser Lithotripsy under Ureteroscopy. *Practical Clinical Medicine*, 17(06): 84–87.
- [3] Hu X, Xia Q, Li X, et al., 2015, Study on the Effect of Body Temperature Flushing Solution on the Body Temperature of Patients Undergoing Percutaneous Nephrolithotomy with Holmium Laser Lithotripsy. *Chinese Journal of Ethnic and Folk Medicine*, 24(03): 110 + 112.

Publisher’s note

Bio-Byword Scientific Publishing remains neutral with regard to jurisdictional claims in published maps and institutional affiliations.



Integrated Services Platform of International Scientific Cooperation

Innoscience Research (Malaysia), which is global market oriented, was founded in 2016. Innoscience Research focuses on services based on scientific research. By cooperating with universities and scientific institutes all over the world, it performs medical researches to benefit human beings and promotes the interdisciplinary and international exchanges among researchers.

Innoscience Research covers biology, chemistry, physics and many other disciplines. It mainly focuses on the improvement of human health. It aims to promote the cooperation, exploration and exchange among researchers from different countries. By establishing platforms, Innoscience integrates the demands from different fields to realize the combination of clinical research and basic research and to accelerate and deepen the international scientific cooperation.

Cooperation Mode



Clinical Workers



In-service Doctors



Foreign Researchers



Hospital



University



Scientific institutions

OUR JOURNALS



The *Journal of Architectural Research and Development* is an international peer-reviewed and open access journal which is devoted to establish a bridge between theory and practice in the fields of architectural and design research, urban planning and built environment research.

Topics covered but not limited to:

- Architectural design
- Architectural technology, including new technologies and energy saving technologies
- Architectural practice
- Urban planning
- Impacts of architecture on environment

Journal of Clinical and Nursing Research (JCNR) is an international, peer reviewed and open access journal that seeks to promote the development and exchange of knowledge which is directly relevant to all clinical and nursing research and practice. Articles which explore the meaning, prevention, treatment, outcome and impact of a high standard clinical and nursing practice and discipline are encouraged to be submitted as original article, review, case report, short communication and letters.

Topics covered by not limited to:

- Development of clinical and nursing research, evaluation, evidence-based practice and scientific enquiry
- Patients and family experiences of health care
- Clinical and nursing research to enhance patient safety and reduce harm to patients
- Ethics
- Clinical and Nursing history
- Medicine



Journal of Electronic Research and Application is an international, peer-reviewed and open access journal which publishes original articles, reviews, short communications, case studies and letters in the field of electronic research and application.

Topics covered but not limited to:

- Automation
- Circuit Analysis and Application
- Electric and Electronic Measurement Systems
- Electrical Engineering
- Electronic Materials
- Electronics and Communications Engineering
- Power Systems and Power Electronics
- Signal Processing
- Telecommunications Engineering
- Wireless and Mobile Communication

